characteristics of 24 NSCLC patients with elevated serum proGRP concentrations. Positive IHC staining for neuroendocrine differentiation was reported in only 4 of 24 serum proGRP-positive NSCLCs, and a small-cell component or neuroendocrine differentiation was detected in all 4 of those patients [13].

In the present study, 27 cytological specimens were reevaluated and IHC staining was performed on 17 histological specimens out of 34 serum proGRP-positive NSCLCs. The cytology results showed the presence of neuroendocrine features such as rosette-like formations in the analysis of 1 squamous cell carcinoma and 5 LCNECs. Histologic examination also identified 2 cases with neuroendocrine morphology (i.e., LCNEC). In addition, weakly or strongly positive staining for some neuroendocrine markers was observed in 12 of 17 histological specimens.

Previous reports have suggested that renal failure can be a source of false-positive proGRP results [11,14], and serum proGRP concentrations were elevated in patients who had serum creatinine levels greater than 1.6 mg/dL [7,13,15]. Therefore, the elevation of serum proGRP detected in present study could be associated with renal dysfunction in the patients analyzed. However, the serum creatinine levels were less than 1.2 mg/dL (median, 0.7 mg/dL) in all 34 serum proGRP-positive NSCLC patients Furthermore, no correlation was observed between serum creatinine and serum proGRP concentrations (data not shown). These results indicate that renal dysfunction could not have accounted for the serum proGRP elevations seen in the present study.

Recently, several reports have suggested that the clinical features of NSCLC with neuroendocrine differentiation, such as LCNEC, may be different from other types of NSCLC [3,16]. The clinical characteristics of serum proGRP-positive NSCLCs were similar to those of SCLCs, as suggested by data showing that the majority of patients were male and heavy smokers. The response rate to platinum-doublet chemotherapy in the present study was 55.0%. This response rate seems higher than the response rates to platinum-doublet chemotherapy reported for nonselected NSCLC [17,18] and serum ProGRP-negative NSCLC in this study, but they were similar to the previously reported response rates to platinum-doublet chemotherapy in LCNEC [16,19]. These results suggest that the sensitivity to chemotherapy in serum proGRP-positive NSCLC may be different than that of other types of NSCLC.

In the present study, IHC staining and a morphologic description were not performed in NSCLC patients with non-elevated proGRP. Therefore, the number of false-negative results and the real performance of the proGRP assay in the detection of neuroendocrine differentiation remain unknown. However, the difficulty in obtaining sufficient tissue by biopsy, and limited tumor tissue sampling make the accurate diagnosis of neuroendocrine differentiation in NSCLC complicated. Sensitive and simple methods for the detection of neuroendocrine differentiation of NSCLC are greatly desired.

In conclusion, serum proGRP-positive NSCLCs may contain manifest neuroendocrine differentiation. In addition, serum proGRP-positive NSCLC patients may have different clinical characteristics compared to other NSCLC patients

Conflict of interest statement

The authors declare no conflicts of interest.

Acknowledgements

The study was conducted by the Cancer Institute Hospital, Japanese Foundation for Cancer Research and Cancer Institute. We thank all investigators in our group.

References

[1] The editorial board of the cancer statistics in Japan. Foundation for Promotion of Cancer Research; October 1, 2007. p. 11–49.
[2] Travis WD, Corrin B, Shimosato Y, Brambilla E.Histological typing of lung and pleural tumors. 3rd ed. Berlin, Heildelberg, Germany: Springer-Verlg; 1999.
[3] Iyoda A, Hiroshima K, Toyozaki T, Haga Y, Fujisawa T, Ohwada H. Clinical characterization of pulmonary large cell neuroendocrine carcinoma and large cell carcinoma with neuroendocrine morphology. Cancer 2001;91: 1992–2000.
[4] Takei H, Asamura H, Maeshima A, Suzuki K, Kondo H, Niki T, et al. Large cell neuroendocrine carcinoma of the lung: a clinicopathologic study of eighty-seven cases. J Thorac Cardiovasc Surg 2002;124:285–92.
[5] Travis WD, Linnoila RI, Tsokos MG, Hitchcock CL, Cutler Jr GB, Nieman L, et al. Neuroendocrine tumors of the lung with proposed criteria for large-cell neuroendocrine carcinoma. An ultrastructural, immunohistochemical, and flow cytometric study of 35 cases. Am J Surg Pathol 1991;15:529–53.
[6] Miyake Y, Kodama T, Yamaguchi K. Pro-gastrin-releasing peptide(31–98) is a specific tumor marker in patients with small cell lung carcinoma. Cancer Res 1994;54:2136–40.
[7] Nakahama H, Tanaka Y, Fujita Y, Fujii M, Sugita M. CYFRA 21-1 and ProGRP, tumor markers of lung cancer, are elevated in chronic renal failure patients. Respirology 1998;3:207–10.
[8] Kodama T, Abe S, Yamaguchi K, Eguchi K, Saigenji K, Kameya T, et al. Clinical significance for diagnosis of serum ProGRP by enzyme-linked immunosorbent assay (ELISA) [in Japanese]. Igaku To Yakugaku 1994;32:87–97.
[9] Holst JJ, Hansen M, Bork E, Schwartz TW. Elevated plasma concentrations of C-flanking gastrin-releasing peptide in small-cell lung cancer. J Clin Oncol 1989;7:1831–8.
[10] Yamaguchi K, Aoyagi K, Urakami K, Fukutani T, Maki N, Yamamoto S, et al. Enzyme-linked immunosorbent assay of pro-gastrin-releasing peptide for small cell lung cancer patients in comparison with neuron-specific enolase measurement. Jpn J Cancer Res 1995;86:698–705.
[11] Molina R, Auge JM, Alicarte J, Filella X, Vinolas N, Ballesta AM. Pro-gastrin-releasing peptide in patients with benign and malignant diseases. Tumour Biol 2004;25:56–61.
[12] Takada M, Kusunoki Y, Masuda N, Matui K, Yana T, Ushijima S, et al. Pro-gastrin-releasing peptide (31–98) as a tumour marker of small-cell lung cancer: comparative evaluation with neuron-specific enolase. Br J Cancer 1996;73:1227–32.
[13] Goto K, Kodama T, Hojo F, Kubota K, Kakinuma R, Matsumoto T, et al. Clinicopathologic characteristics of patients with nonsmall cell lung carcinoma with elevated serum progastrin-releasing peptide levels. Cancer 1998;82: 1056–61.
[14] Casesa A, Filellab X, Molinab R, Ballestab AM, Lopez-Pedreta J, Reverta L. Tumor markers in chronic renal failure and hemodialysis patients. Nephron 1991;57:183–6.
[15] Kamata K, Uchida M, Takeuchi Y, Takahashi E, Sato N, Miyake Y, et al. Increased serum concentrations of pro-gastrin-releasing peptide in patients with renal dysfunction. Nephrol Dial Transplant 1996;11:1267–70.
[16] Fujiwara Y, Sekine I, Tsuta K, Ohe Y, Kunitoh H, Yamamoto N, et al. Effect of platinum combined with irinotecan or paclitaxel against large cell neuroendocrine carcinoma of the lung. Jpn J Clin Oncol 2007;37:482–6.
[17] Ohe Y, Ohashi Y, Kubota K, Tamura T, Nakagawa K, Negoro S, et al. Randomized phase III study of cisplatin plus irinotecan versus carboplatin plus paclitaxel, cisplatin plus gemcitabine, and cisplatin plus vinorelbine for advanced non-small-cell lung cancer: four-arm cooperative study in japan. Ann Oncol 2007;18:317–23.
[18] Schiller JH, Harrington D, Belani CP, Langer C, Sandler A, Krook J, et al. Comparison of four chemotherapy regimens for advanced non-small-cell lung cancer. N Engl J Med 2002;346:92–8.
[19] Yamazaki S, Sekine I, Matsuno Y, Takei H, Yamamoto N, Kunitoh H, et al. Clinical responses of large cell neuroendocrine carcinoma of the lung to cisplatin-based chemotherapy. Lung Cancer 2005;49:217–23.

nature medicine

RET, ROS1 and ALK fusions in lung cancer

Kengo Takeuchi[1,2], Manabu Soda[3], Yuki Togashi[1,2], Ritsuro Suzuki[4], Seiji Sakata[1], Satoko Hatano[1], Reimi Asaka[1,2], Wakako Hamanaka[2], Hironori Ninomiya[2], Hirofumi Uehara[5], Young Lim Choi[6], Yukitoshi Satoh[5,7], Sakae Okumura[5], Ken Nakagawa[5], Hiroyuki Mano[3,6] & Yuichi Ishikawa[2]

Through an integrated molecular- and histopathology-based screening system, we performed a screening for fusions of anaplastic lymphoma kinase (ALK) and c-ros oncogene 1, receptor tyrosine kinase (ROS1) in 1,529 lung cancers and identified 44 ALK-fusion–positive and 13 ROS1-fusion–positive adenocarcinomas, including for unidentified fusion partners for ROS1. In addition, we discovered previously unidentified kinase fusions that may be promising for molecular-targeted therapy, kinesin family member 5B (KIF5B)-ret proto-oncogene (RET) and coiled-coil domain containing 6 (CCDC6)-RET, in 14 adenocarcinomas. A multivariate analysis of 1,116 adenocarcinomas containing these 71 kinase-fusion–positive adenocarcinomas identified four independent factors that are indicators of poor prognosis: age ≥50 years, male sex, high pathological stage and negative kinase-fusion status.

Echinoderm microtubule associated protein like 4 (EML4)-ALK was the first targetable fusion oncokinase to be identified in non–small cell lung cancer (NSCLC)[1]. This fusion is found in approximately 4–6% of lung adenocarcinomas[2,3]. ROS1 is another receptor tyrosine kinase that forms fusions in NSCLC[4]. Solute carrier family 34 (sodium phosphate), member 2 (SLC34A2)-ROS1 and CD74 molecule, major histocompatibility complex, class II invariant chain (CD74)-ROS1 were identified in 1 out of 41 NSCLC cell lines and 1 out of 150 lung cancer samples, respectively[4]. However, the oncogenic ability of these ROS1 fusion proteins and the incidence of ROS1 fusions in lung cancers are still unclear.

We screened for known and unknown kinase fusions in lung cancers using a histopathology-based system with tissue microarrays of 1,528 surgically removed tissues (**Supplementary Methods** and **Supplementary Appendix**). Immunohistochemistry of antibodies to ALK using the intercalated antibody-enhanced polymer method[2,3,5–7] detected 45 tumors with ALK kinase domain expression (**Supplementary Fig. 1**). In 44 adenocarcinomas, multiplex RT-PCR[2,3] identified 41 *EML4-ALK*–positive and 3 *KIF5B-ALK*–positive adenocarcinomas, including a previously unidentified KIF5B-ALK fusion variant, K17;A20 (**Supplementary Table 1**). Further, we used fluorescence *in situ* hybridization (FISH) for split and fusion assays to confirm the presence of ALK fusions[2,3,8]. The FISH results for the *ALK* split assay, the *EML4-ALK* fusion assay and the *KIF5B-ALK* fusion assay in the 44 adenocarcinomas were all consistent with the presence of the corresponding fusion gene (**Supplementary Figs. 2** and **3**). The remaining tumor that was positive for antibodies to ALK as determined by immunohistochemistry (a large-cell neuroendocrine carcinoma) was negative in the FISH assays and expressed wild-type ALK. ALK fusions existed in 3.0% (44 out of 1,485) of the NSCLCs and 3.9% (44 out of 1,121) of the adenocarcinomas. We included 20 previously reported ALK-fusion–positive and 304 ALK-fusion–negative tumors, all of which were screened with multiplex RT-PCR. Because specimens of these 324 patients were collected consecutively during the period of tissue collection, they served as positive and negative controls, respectively[1–3,8,9]. The immunohistochemistry results using the intercalated antibody-enhanced polymer method were complete matches in the 20 fusion-positive and the 304 fusion-negative tumors.

We used split FISH assays for the screening for *ROS1* gene rearrangement (**Fig. 1**). In 11 of the 13 *ROS1* split FISH-positive tumors (**Fig. 1a**), 5′ rapid amplification of complementary DNA ends (5′ RACE) identified two known and three unknown fusion partners for *ROS1*: *TPM3*, *SDC4*, *SLC34A2*, *CD74* and *EZR* (**Fig. 1b** and **Supplementary Table 1**); RT-PCR confirmed this finding (**Fig. 1c**). In a 5′-RACE–negative tumor (ROS#12) (again, where split FISH is used to detect candidate fusion genes of interest by the presence of rearrangements and RACE is used for the identification of fusion partners), each fusion-specific RT-PCR (using a common reverse primer) amplified the same band, which contained an *LRIG3* sequence. This tumor was proven fusion-positive in RT-PCR specific to *LRIG3-ROS1*, an unidentified fusion. Fusion FISH results confirmed that all 12 cases harbored the corresponding fusion (**Fig. 1a**). All fusion FISH assays for these six ROS1 fusions were negative for the tumor ROS#13 (the frozen material had been consumed), indicating an unknown fusion partner for *ROS1*. *ROS1* split FISH screening failed for nine NSCLCs, including five adenocarcinomas. We identified ROS1 fusions in 0.9% (13 out of 1,476) of the NSCLCs and 1.2% (13 out of 1,116) of the adenocarcinomas.

We performed *KIF5B* split FISH to discover new fusion kinases, as we previously identified KIF5B-ALK fusions in lung cancer[3]. As such, we hypothesized that KIF5B might be rearranged in lung cancer. In 24 *KIF5B* split FISH-positive tumors, 3′ RACE identified an in-frame fusion between *KIF5B* exon 23 and *RET* exon 12

[1]Pathology Project for Molecular Targets, the Cancer Institute, Japanese Foundation for Cancer Research, Tokyo, Japan. [2]Division of Pathology, the Cancer Institute, Japanese Foundation for Cancer Research, Tokyo, Japan. [3]Division of Functional Genomics, Jichi Medical University, Tochigi, Japan. [4]Department of Hematopoietic Stem Cell Transplantation Data Management and Biostatistics, Nagoya University Graduate School of Medicine, Nagoya, Japan. [5]Department of Thoracic Surgical Oncology, Thoracic Center, the Cancer Institute Hospital, Japanese Foundation for Cancer Research, Tokyo, Japan. [6]Department of Medical Genomics, Graduate School of Medicine, University of Tokyo, Tokyo, Japan. [7]Present address: Department of Thoracic Surgery, Kitasato University School of Medicine, Kanagawa, Japan. Correspondence should be addressed to K.T. (kentakeuchi-tky@umin.net).

Received 28 September 2011; accepted 3 January 2012; published online 12 February 2012; doi:10.1038/nm.2658

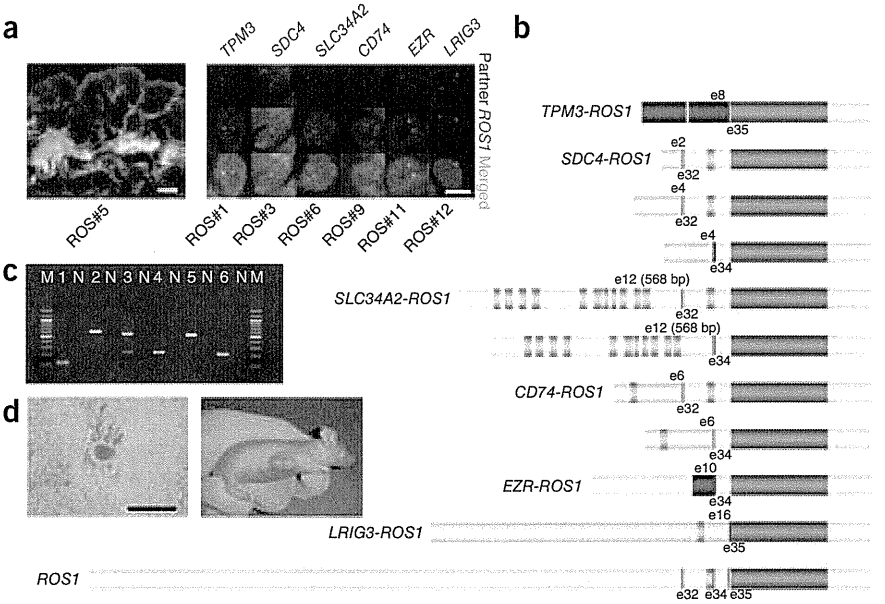

Figure 1 Identification of ROS1 fusions. (**a**) *ROS1* split (left) and fusion (right) FISH assay data (scale bars, 20 μm). In the split assay, multiple tumor cells harbored individual 3′ side signals (green), indicating the presence of a *ROS1* rearrangement. In the fusion assay, a fusion signal (yellow) was observed in the representative tumor cell of each subject, which is consistent with the presence of t(1;6)(q21.2;q22) for *TPM3-ROS1*, t(6;20)(q22;q12) for *SDC4-ROS1*, t(4;6)(q15.2;q22) for *SLC34A2-ROS1*, t(5;6)(q32;q22) for *CD74-ROS1*, inv(6)(q22q25.3) for *EZR-ROS1* or t(6;12)(q22;q14.1) for *LRIG3-ROS1*. (**b**) The break points of ROS1 are exons 32, 34 and 35. All of the break points allow the resulting fusion to harbor the kinase domain of ROS1 (red), and the exon 32 break point allows the resulting fusion to harbor the transmembrane domain of ROS1 (orange). In the fusion partners, dark blue and orange represent coiled-coil and transmembrane domains, respectively. Coiled-coil domains may contribute to homodimelization, but only TPM3 and EZR contained these domains. In contrast to ALK and RET fusions, the role of the fusion partner's coiled-coil domain is unknown in ROS1 fusions. e, exon. (**c**) Results for fusion-specific RT-PCR for tumors ROS#1 (lane 1, TPM3-ROS1, T8;R35, predicted product size of 119 bp), ROS#3 (lane 2, SDC4-ROS1, S2;R32, 596 bp), ROS#6 (lane 3, SLC34A2-ROS1, S13del2046;R32 and S13del2046;R34, 544 bp and 235 bp, respectively), ROS#8 (lane 4, CD74-ROS1, C6;R34, 230 bp), ROS#10 (lane 5, EZR-ROS1, E10;R34, 527 bp), and ROS#12 (lane 6, LRIG3-ROS1, L16;R35, 218 bp). M and N represent the size marker (100-bp ladder) and the non-template control, respectively. (**d**) The transforming potential of the ROS1 fusion. Mouse 3T3 fibroblasts infected with a retrovirus encoding SDC4-ROS1 derived from tumor ROS#4 formed multiple foci (scale bar, 1 mm). All of the four nude mice injected with the corresponding 3T3 cells developed a subcutaneous tumor (right).

(tumor RET#11). *RET* split FISH on the tissue arrays identified 22 fusion-positive tumors in 1,528 lung cancers (**Fig. 2a**), from which a multiplex RT-PCR system that captures all possible *KIF5B-RET* fusions detected 12 fusion-positive tumors: eight tumors with the fusion of *KIF5B* exon 15 and *RET* exon 12 (K15;R12) and one tumor each with the K16;R12, K22;R12, K23;R12 and K24;R11 fusions (**Fig. 2b** and **Supplementary Table 1**). The *KIF5B-RET* fusion FISH results were consistent with the presence of inv(10)(p11.22q11.2) in all 12 of these tumors (**Fig. 2a**).

In a routine histopathological diagnosis, we encountered an adenocarcinoma that showed a mucinous cribriform pattern (**Fig. 2c**) that was previously reported as a histopathological marker for the presence of EML4-ALK (**Supplementary Fig. 4**)[9–11]. Notably, this adenocarcinoma (tumor RET#14) was negative for ALK fusion and was positive for *CCDC6-RET*, as determined by FISH and inverse RT-PCR; the latter fusion gene was first described in thyroid cancer[12]. RT-PCR identified another tumor positive for the *CCDC6-RET* fusion (RET#13) in the remaining 10 tumors. The 14 RET-positive tumors (out of the total 1,528 tumors tested, with one additional tumor (RET#14) found through routine pathology diagnostic service) were also positive in the revised multiplex RT-PCR that captured *EML4-ALK*, *KIF5B-ALK*, *KIF5B-RET* and *CCDC6-RET* simultaneously (**Fig. 2d**). The RET kinase domain expression using real-time RT-PCR was weak or undetectable for the remaining nine tumors determined to be positive in the *RET* split FISH screening. Perhaps the genomic rearrangement occurred downstream of the *RET* break points. *RET* split FISH screening failed in three NSCLCs, including two adenocarcinomas. RET#14 was the index case found in routine pathology diagnostic service but not in the 1,528 cohort. RET fusions existed in 0.9% (13 out of 1,482) of the NSCLCs and 1.2% (13 out of 1,119) of the adenocarcinomas. The 14 RET fusion-positive subjects did not receive vandetanib.

We concluded that the rearrangements described above are somatic without using any matched normal tissues. Our histopathology-based screening method preserves the samples' histological architecture. This allows observers to confirm that internal non-tumor cells, for example, epithelial cells, inflammatory cells or fibroblasts, are negative in a test of interest.

All 71 kinase-fusion–positive (44 ALK, 13 ROS1 and 14 RET fusions) lung cancers were exclusively adenocarcinomas (6% of all adenocarcinomas in the present study), were positive for antibodies to TTF1, which is regarded as a marker for lung adenocarcinoma, as determined by immunohistochemistry (excluding two ALK-positive tumors) and were negative for *EGFR* and *KRAS* mutations. Thirteen of the 44 ALK-positive tumors (30%) were weakly positive for p63 expression (were weakly positive for a squamous cell carcinoma marker, p63) (**Supplementary Table 1**). Thirty-three tumors showed a mucinous cribriform pattern in at least 5% of their area; 22 tumors had this pattern in >25% of their area (**Fig. 2c, Supplementary Table 1** and **Supplementary Fig. 4**). The frequency of mucinous cribriform carcinoma was significantly higher in the kinase-fusion–positive group of tumors than in the 77 fusion-negative adenocarcinomas (22 out of 71 compared to 7 out of 77, respectively; $P = 0.00088$). Notably, we observed this pattern preferentially in EML4-ALK–positive tumors (70%, 29 out of 41); all three CD74-ROS1–positive tumors also showed this pattern. Recognizing this pattern in routine pathology diagnoses led to the identification of the CCDC6-RET fusion (tumor RET#14). In organs other than the lung, secretory breast carcinoma, which is characterized by a cribriform pattern with abundant secretory material, harbors the ets variant 6 (ETV6)-neurotrophic tyrosine kinase, receptor, type 3 (NTRK3) fusion (ref. 13). We identified an ALK-fusion–positive renal cell carcinoma that showed a mucinous cribriform pattern[7]. This pattern may be linked to the presence of particular kinase fusions[10], and this possibility warrants further study.

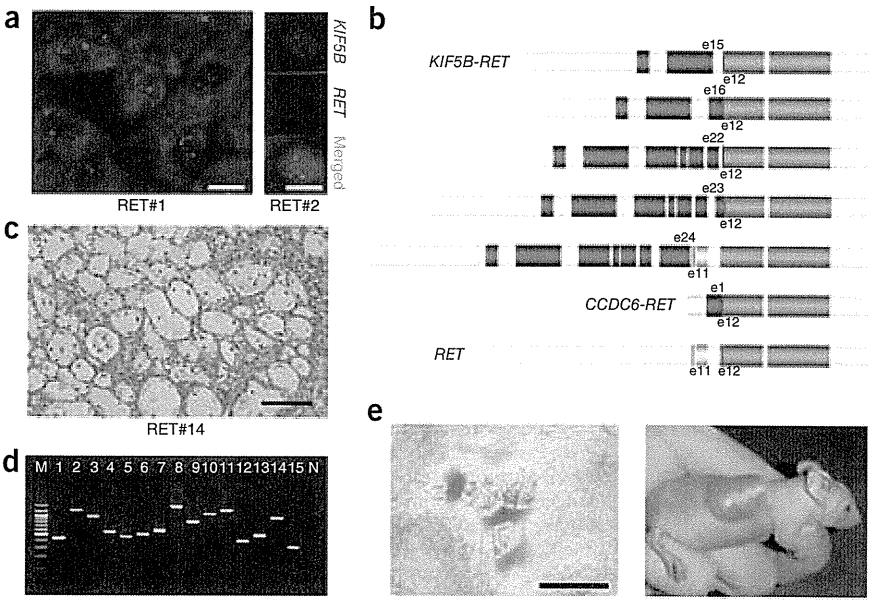

Figure 2 Discovery of RET fusions. (**a**) *RET* split (left) and fusion (right) FISH assay data (scale bars, 20 μm). In the split assay, multiple tumor cells harbored individual 3′ side signals (green), indicating the presence of *RET* rearrangement. In the fusion assay, a fusion signal (yellow) was observed in the representative tumor cell of subject RET#2, which is consistent with the presence of inv(10)(p11.22q11.2). (**b**) The break points of RET are exons 11 and 12. Both of the break points allow the resulting fusion to harbor the kinase domain of RET (red), and the exon 11 break point allows the resulting fusion to harbor the transmembrane domain of RET (orange). In the fusion partners, dark blue represents a coiled-coil domain, which probably contributes to the homodimelization of the fusion. Only the longer isoforms of RET and the RET fusions are shown. (**c**) Subject RET#14 showed the representative histopathology of mucinous cribriform carcinoma (scale bar, 100 μm). (**d**) The results for fusion-specific RT-PCR for subjects ALK#10 (lane 1, EML4-ALK, E13;A20, predicted product size of 432 bp), ALK#16 (lane 2, EML4-ALK, E20;A20, 1185 bp), ALK#26 (lane 3, EML4-ALK, E6;A20, 913 bp), ALK#38 (lane 4, EML4-ALK, E14;ins11del49A20, 546 bp), ALK#39 (lane 5, EML4-ALK, E2;A20, 454 bp), ALK#40 (lane 6, EML4-ALK, E13;ins69A20, 501 bp), ALK#41 (lane 7, EML4-ALK, E14;del14A20, 570 bp), ALK#42 (lane 8, KIF5B-ALK, K17;A20, 1,483 bp), ALK#44 (lane 9, KIF5B-ALK, K24;A20, 814 bp), RET#6 (lane 10, KIF5B-RET, K15;R12, 1,104 bp), RET#9 (lane 11, KIF5B-RET, K16;R12, 1,293 bp), RET#10 (lane 12, KIF5B-RET, K22;R12, 420 bp), RET#11 (lane 13, KIF5B-RET, K23;R12, 525 bp), RET#12 (lane 14, KIF5B-RET, K24;R11, 999 bp) and RET#13 (lane 15, CCDC6-RET, C1;R12, 352 bp). M and N represent the size marker (100-bp ladder) and non-template control, respectively. (**e**) The transforming potential of the KIF5B-RET fusion. Mouse 3T3 fibroblasts infected with a retrovirus encoding K15;R12L derived from tumor RET#7 fomed multiple foci (scale bar, 1 mm). All of the four nude mice injected with the corresponding 3T3 cells developed a subcutaneous tumor (right).

Supplementary Tables 1–4 summarize the clinicopathological features of the subjects. Briefly, young age, low smoking index and small tumor size characterized the kinase-fusion–positive group of subjects (**Supplementary Table 2**). A multivariate analysis of the adenocarcinomas revealed four independent factors that were indicators of poor prognosis: age ≥50 years, male sex, high pathological stage and negative kinase-fusion status (**Supplementary Table 3**). There was no significant difference in overall survival between the kinase-positive and epidermal growth factor receptor (EGFR)-mutant groups (P = 0.32). **Supplementary Table 4** shows the clinicopathological features of the subjects stratified by each fusion.

The transforming ability of CCDC6-RET and all of the ALK fusions, excluding K17;A20, was shown previously[1–3,8,12]. 3T3 cells infected with a virus expressing K17;A20, tropomyosin 3 (TPM3)-ROS1, syndecan 4 (SDC4)-ROS1, SLC34A2-ROS1, CD74-ROS1, ezrin (EZR)-ROS1, leucine-rich repeats and immunoglobulin-like domains 3 (LRIG3) (transcript variant 2)-ROS1 or KIF5B-RET (with both the longer (RET51) and shorter (RET9) RET isoforms) led to multiple transformed foci formation in culture and in subcutaneous tumors in a nude mouse tumorigenicity assay (**Figs. 1d, 2e** and **Supplementary Fig. 5**).

To test whether vandetanib, an inhibitor of vascular endothelial growth factor receptor (VEGFR-2), VEGFR-3, EGFR and RET[14], might be effective for the treatment of RET-fusion–positive tumors, we induced Flag-tagged EML4-ALK (E13;A20) or KIF5B-RET (K15;R12L and K15;R12S) in Ba/F3 cells, which are dependent on interleukin-3 (IL-3) for growth. All transfected cells, including those without any kinase fusion, proliferated in the presence of IL-3, but only cells expressing E13;A20 or K15;R12L grew in the absence of IL-3 (**Supplementary Fig. 6a**). In the absence of IL-3, vandetanib inhibited the proliferation of cells expressing K15;R12L (**Supplementary Fig. 6c**) but not the proliferation of cells expressing E13;A20 (**Supplementary Fig. 6d**). Crizotinib was not effective in inhibiting the proliferation of Ba/F3 cells expressing K15;R12L (**Supplementary Fig. 7**).

In 1985, a 3T3 assay identified *RET* as a rearranged transforming gene[15]. RET fusions have been identified exclusively in papillary thyroid carcinoma and are more frequently observed in radiation-associated thyroid cancers (for example, in survivors of the Chernobyl accident[16], atomic bomb survivors[17] and post-radiation therapy patients[18]). Therefore, a retrospective comparison of RET fusions in individuals with lung cancer with and without a history of radiation exposure warrants further study. If a positive association is found between RET fusion and radiation exposure in these studies, it might be desirable for individuals with internal or therapeutic exposure to irradiation (for example, those individuals involved in the Fukushima accident) to be monitored prospectively for lung cancer as well as thyroid cancer.

In Japan, more than 40% of lung adenocarcinomas in younger individuals harbor EGFR mutations[19]. In this study, 16% (17 out of 107) of younger individuals (≤50 years of age) with adenocarcinoma harbored a kinase fusion. Collectively, as long as molecular target diagnoses are properly performed, >50% of the individuals with lung adenocarcinoma in this generation may benefit from treatment with corresponding kinase inhibitors. Integrated pathology-based screening techniques can also be used for the selection of individuals to receive this treatment[20]. The results of our study will facilitate the development of a molecular classification of lung adenocarcinomas that is closely related to both the pathogenesis and the treatment of disease. This study was approved by the Institutional Review Board of the Cancer Institute Hospital, and all subjects provided informed consent.

METHODS

Methods and any associated references are available in the online version of the paper at http://www.nature.com/naturemedicine/.

Note: Supplementary information is available on the Nature Medicine website.

ACKNOWLEDGMENTS

We thank M. Iwakoshi, K. Shiozawa, T. Kakita, H. Nagano and K. Nomura for their technical assistance and S. Sengoku for providing administrative assistance. This work was supported in part by Grants-in-Aid for Scientific Research from the Ministry of Education, Culture, Sports, Science and Technology of Japan, as well as by grants from the Japan Society for the Promotion of Science; the Ministry of Health, Labor and Welfare of Japan; the Vehicle Racing Commemorative Foundation of Japan; the Princess Takamatsu Cancer Research Fund; and the Uehara Memorial Foundation.

AUTHOR CONTRIBUTIONS

K.T. conceived of and led the entire project, designed the FISH probes, screened samples using FISH and immunohistochemistry, performed histopathological analyses, generated figures and tables and wrote the manuscript. M.S. performed functional analyses and generated the figures. Y.T. performed inverse RT-PCR and RACE experiments and their corresponding analyses. R.S. conducted statistical analyses. S.S. performed FISH and histopathological analyses. S.H. processed and analyzed the tissue microarrays and FISH screening and generated figures. R.A. processed the FISH probe library. W.H. made and analyzed the database and processed tissue microarrays. H.N., H.U., Y.S., S.O. and K.N. collected specimens and clinical information and were involved in planning the project. Y.L.C. conducted functional analyses. H.M. supervised the functional analyses and planned the project. Y.I. performed histopathological analyses and collected specimens. All authors participated in the discussion and interpretation of the data and the results.

COMPETING FINANCIAL INTERESTS

The authors declare no competing financial interests.

Published online at http://www.nature.com/naturemedicine/.
Reprints and permissions information is available online at http://www.nature.com/reprints/index.html.

1. Soda, M. *et al. Nature* **448**, 561–566 (2007).
2. Takeuchi, K. *et al. Clin. Cancer Res.* **14**, 6618–6624 (2008).
3. Takeuchi, K. *et al. Clin. Cancer Res.* **15**, 3143–3149 (2009).
4. Rikova, K. *et al. Cell* **131**, 1190–1203 (2007).
5. Takeuchi, K. *et al. Haematologica* **96**, 464–467 (2011).
6. Takeuchi, K. *et al. Clin. Cancer Res.* **17**, 3341–3348 (2011).
7. Sugawara, E. *et al. Cancer* published online, doi:10.1002/cncr.27391 (17 January 2012).
8. Choi, Y.L. *et al. Cancer Res.* **68**, 4971–4976 (2008).
9. Inamura, K. *et al. J. Thorac. Oncol.* **3**, 13–17 (2008).
10. Takeuchi, K. *Pathol. and Clin. Med.* **28**, 139–144 (2010).
11. Jokoji, R. *et al. J. Clin. Pathol.* **63**, 1066–1070 (2010).
12. Grieco, M. *et al. Cell* **60**, 557–563 (1990).
13. Tognon, C. *et al. Cancer Cell* **2**, 367–376 (2002).
14. Flanigan, J., Deshpande, H. & Gettinger, S. *Biologics* **4**, 237–243 (2010).
15. Takahashi, M., Ritz, J. & Cooper, G.M. *Cell* **42**, 581–588 (1985).
16. Ito, T. *et al. Lancet* **344**, 259 (1994).
17. Hamatani, K. *et al. Cancer Res.* **68**, 7176–7182 (2008).
18. Bounacer, A. *et al. Oncogene* **15**, 1263–1273 (1997).
19. Kosaka, T. *et al. Cancer Res.* **64**, 8919–8923 (2004).
20. Han, B. *et al. Cancer Res.* **68**, 7629–7637 (2008).

Original Article

Identification of Anaplastic Lymphoma Kinase Fusions in Renal Cancer

Large-Scale Immunohistochemical Screening by the Intercalated Antibody-Enhanced Polymer Method

Emiko Sugawara, MD[1,2]; Yuki Togashi, MS[1,3]; Naoto Kuroda, MD[4]; Seiji Sakata, MD, PhD[1]; Satoko Hatano, BS[1,3]; Reimi Asaka, BS[1,3]; Takeshi Yuasa, MD, PhD[5]; Junji Yonese, MD, PhD[5]; Masanobu Kitagawa, MD, PhD[2]; Hiroyuki Mano, MD, PhD[6,7]; Yuichi Ishikawa, MD, PhD[3]; and Kengo Takeuchi, MD, PhD[1,3]

BACKGROUND: Several promising molecular-targeted drugs are used for advanced renal cancers. However, complete remission is rarely achieved, because none of the drugs targets a key molecule that is specific to the cancer, or is associated with "oncogene addiction" (dependence on one or a few oncogenes for cell survival) of renal cancer. Recently, an anaplastic lymphoma kinase (ALK) fusion, vinculin-ALK, has been reported in pediatric renal cell carcinoma (RCC) cases who have a history of sickle cell trait. In this context, ALK inhibitor therapy would constitute a therapeutic advance, as has previously been demonstrated with lung cancer, inflammatory myofibroblastic tumors, and anaplastic large cell lymphomas. **METHODS:** Anti-ALK immunohistochemistry was used to screen 355 tumor tissues, using the intercalated antibody-enhanced polymer (iAEP) method. The cohort consisted of 255 clear cell RCCs, 32 papillary RCCs, 34 chromophobe RCCs, 6 collecting duct carcinomas, 10 unclassified RCCs, 6 sarcomatoid RCCs, and 12 other tumors. **RESULTS:** Two patients (36- and 53-year-old females) were positive for ALK as determined by iAEP immunohistochemistry. Using 5′-rapid amplification of complementary DNA ends, we detected *TPM3-ALK* and *EML4-ALK* in these tumors. The results of this study were confirmed by fluorescence in situ hybridization assays. The 2 ALK-positive RCCs were unclassified (mixed features of papillary, mucinous cribriform, and solid patterns with rhabdoid cells) and papillary subtype. They comprised 2.3% of non-clear cell RCCs (2 of 88) and 3.7% of non-clear cell and nonchromophobe RCCs (2 of 54). **CONCLUSIONS:** The results of this study indicate that ALK fusions also exist in adult RCC cases without uncommon backgrounds. These findings confirm the potential of ALK inhibitor therapy for selected cases of RCC. ***Cancer* 2012;000:000-000.** © *2012 American Cancer Society.*

KEYWORDS: anaplastic lymphoma kinase, molecular-targeted therapy, renal cell carcinoma, immunohistochemistry, intercalated antibody-enhanced polymer.

INTRODUCTION

Renal cancer is one of the major cancers. The incidence and mortality of cases are estimated at 273,518 and 116,368 in the world; 14,963 and 6957 in Japan; and 56,678 and 13,711 in the United States.[1] The 5-year survival rate of patients with localized disease is relatively good: 65% to 93% and 47% to 77% for stages 1 and 2, respectively.[2] For advanced renal cancers (34%-80% and 2%-20% 5-year survival rates in stages 3 and 4, respectively),[2] several molecular-targeted drugs have been recently approved by the US Food and Drug Administration. These drugs, which include sunitinib, sorafenib, temsirolimus, everolimus, bevacizumab, pazopanib, and axitinib, are promising. However, none of them targets a key molecule that is specific to the cancer, or is associated with "oncogene addiction" of renal cancer, namely, the dependence on one or a few oncogenes for maintenance of the malignant phenotype and cell survival.

Anaplastic lymphoma kinase (ALK) fusion is a potential vulnerability, an "Achilles' heel", of many types of human cancer, including lymphoma,[3,4] sarcoma,[5] and carcinoma.[6,7] Experimentally, lung adenocarcinomas developed in EML4-ALK (fusion of ALK with echinoderm microtubule–associated protein like 4) transgenic mice were successfully treated with an ALK inhibitor.[8] The ALK inhibitor crizotinib has recently been used in patients with lung cancer, inflammatory myofibroblastic tumors (IMTs), or anaplastic large cell lymphomas (ALCLs), which harbor various ALK fusions. The compound showed an 81% response rate in ALK-positive lung cancers defined by at least 2 diagnostic methods,[9,10] and a

Corresponding author: Kengo Takeuchi, MD, PhD, Pathology Project for Molecular Targets, The Cancer Institute, Japanese Foundation for Cancer Research, 3-8-31 Ariake, Koto, Tokyo 135-8550, Japan; Fax: (81) 3-3570-0230; kentakeuchi-tky@umin.net

[1]Pathology Project for Molecular Targets, The Cancer Institute, Japanese Foundation for Cancer Research, Tokyo, Japan; [2]Department of Comprehensive Pathology, Graduate School, Tokyo Medical and Dental University, Tokyo, Japan; [3]Division of Pathology, The Cancer Institute, Japanese Foundation for Cancer Research, Tokyo, Japan; [4]Department of Diagnostic Pathology, Kochi Red Cross Hospital, Kochi City, Kochi, Japan; [5]Department of Urology, The Cancer Institute Hospital, Japanese Foundation for Cancer Research, Tokyo, Japan; [6]Division of Functional Genomics, Jichi Medical University, Tochigi, Japan; [7]Department of Medical Genomics, Graduate School of Medicine, University of Tokyo, Tokyo, Japan

We thank Tomoyo Kakita, Keiko Shiozawa, and Motoyoshi Iwakoshi for their technical assistance, and Sayuri Sengoku for providing administrative assistance.

DOI: 10.1002/cncr.27391, **Received:** October 1, 2011; **Revised:** October 31, 2011; **Accepted:** November 10, 2011, **Published online** in Wiley Online Library (wileyonlinelibrary.com)

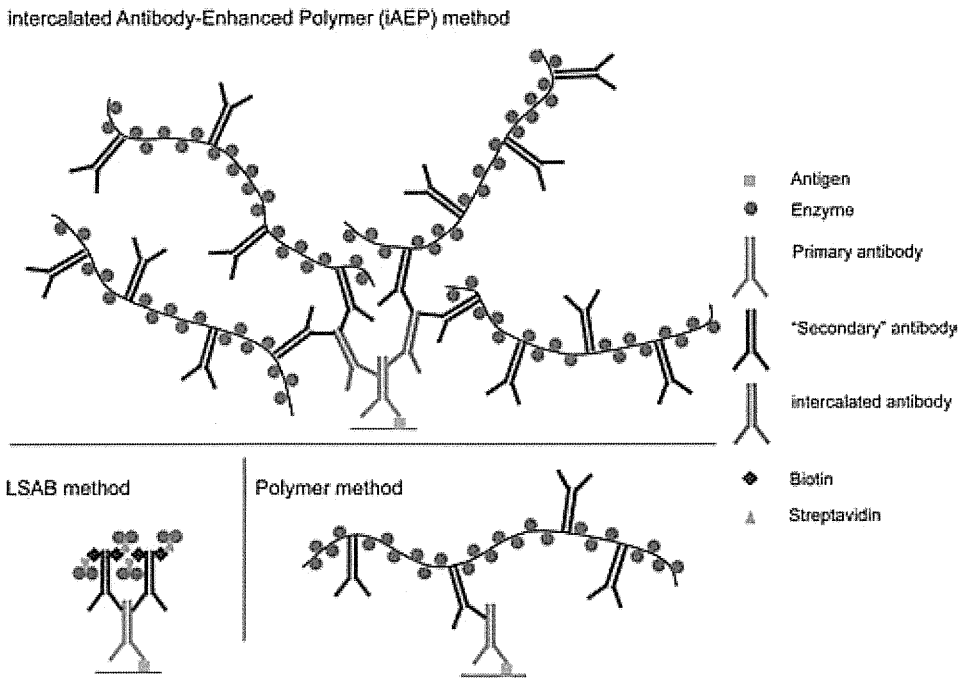

Figure 1. Schematic of intercalated antibody-enhanced polymer (iAEP) method is shown. The labeled streptavidin biotin (LSAB) and polymer methods are common conventional immunohistochemistry methods. In the iAEP method, a step of "intercalated antibody" is added between those of the primary antibody and polymer reagent. Thus, the iAEP method has an additional step compared with the polymer method, but the same number of steps as the LSAB method. There are generally 2 ways to raise the sensitivity of immunohistochemistry. The first is to raise the sensitivity of the antigen-antibody reaction, by increasing the concentration of the primary antibody, using a more sensitive antibody, antigen-retrieval technique, and so forth. The second is to raise the sensitivity of the detection system for the antigen-antibody immune complex. These 2 techniques may appear to generate the same result; however, in principle, they are totally different. The staining results are more likely to differ, especially when the antigen density is very low, such as for EML4-ALK (fusion of echinoderm microtubule-associated protein like 4 with anaplastic lymphoma kinase) or PPFIBP1-ALK (fusion of PTPRF interacting protein binding protein 1 with ALK).[13,24] In such a setting, the latter technique is more advantageous. The staining intensity depends on the density of enzyme in the antigen site. However sensitive a primary antibody is, the antigen-antibody complex cannot exceed the number of antigens. In contrast, it is easy to increase the enzyme density per antigen-antibody complex with use of the latter technique, which includes the iAEP method.

strong response in IMT for several months.[11] Two patients with ALCL who were receiving crizotinib achieved complete remission.[12] These findings indicate that ALK fusion addiction is one of the most promising targets in cancer therapy.

To ensure that such molecular-targeted therapy is effective and less toxic, accurate screening methods to detect ALK fusions are crucial. However, although immunohistochemistry has been a gold standard for the detection of ALK fusions in ALCL and IMT,[13,14] conventional anti-ALK immunohistochemistry is not sensitive enough to detect EML4-ALK, which was first described in lung cancer in 2007.[6,7] To overcome this, we developed a sensitive immunohistochemical tool, the intercalated antibody-enhanced polymer (iAEP) method (Fig. 1).[13] Combined with a conventional anti-ALK mouse monoclonal antibody 5A4, the iAEP method efficiently and consistently detected EML4-ALK in paraffin-embedded sections. In various studies on ALK-positive lung cancer, anti-ALK immunohistochemistry by iAEP or essentially equivalent methods was used to examine surgically resected specimens,[13,15-19] transbronchial lung biopsy specimens,[20] and endobronchial ultrasound-guided transbronchial needle aspiration specimens.[17,21,22] More importantly, some of the patients screened by anti-ALK iAEP immunohistochemical analysis received crizotinib therapy and showed a good response.[16,17,22] Novel ALK fusions, including v6 and v7 of EML4-ALK,[13] kinesin family member 5B (KIF5B)-ALK,[13] sequestosome 1 (SQSTM1)-ALK,[23] and PTPRF interacting protein, binding protein 1 (PPFIBP1)-ALK[24] have been identified using anti-ALK iAEP immunohistochemical analysis. Thus, anti-ALK iAEP immunohistochemistry constitutes a powerful tool for clinical and also research purposes.

The development of anti-ALK antibodies has facilitated the investigation of many types and cases of cancer, including lung cancer.[25-27] Since 1994, ALK-positive tumors have been identified exclusively in lymphoma

(ALCL and ALK-positive large B-cell lymphoma[28]) and sarcoma (IMT,[5] rhabdomyosarcoma,[26] and neuroblastoma[29]). It was not until 2007 that the presence of an ALK fusion was described in lung cancer.[6] This seems to be mainly because EML4-ALK is barely detectable by conventional anti-ALK immunohistochemistry. Considering in reverse, in cases of a tumor that is positive by anti-ALK iAEP immunohistochemistry, but negative by conventional anti-ALK immunohistochemistry, the tumor may have a novel ALK fusion partner, or express wild-type ALK at a modest level. Indeed, in "ALK-negative" IMT cases defined by conventional ALK immunohistochemistry, PPFIBP1-ALK was identified through reassessment for ALK fusions, using anti-ALK iAEP immunohistochemistry.[24] This prompted us to reevaluate other types of solid cancers for ALK fusions. Here, we describe the identification of TPM3-ALK (fusion of tropomyosin 3 and ALK) and EML4-ALK in renal cancer, by anti-ALK iAEP immunohistochemistry.

MATERIALS AND METHODS

Materials

We examined 355 renal tumor tissues from patients who had received surgery in the Cancer Institute Hospital, Japanese Foundation for Cancer Research, Tokyo, between 1994 and 2010. Renal tumors included 255 clear cell renal cell carcinomas (RCCs), 32 papillary RCCs, 34 chromophobe RCCs, 6 collecting duct carcinomas, 10 unclassified RCCs, 6 sarcomatoid RCCs, and 12 other tumors (4 oncocytomas, 3 angiomyolipomas, 1 solitary fibrous tumor, 2 spindle cell sarcomas, 1 desmoplastic sarcoma, and 1 anaplastic carcinoma). Surgically removed tumor specimens were routinely fixed in 20% neutralized formalin and embedded in paraffin for conventional histopathological examination. Immunohistochemical screenings were performed using tissue microarrays. For the 2 cases positive for anti-ALK immunohistochemistry, total RNA was extracted from the corresponding snap-frozen specimen, and purified with the use of an RNeasy Mini kit (Qiagen, Tokyo, Japan). Informed consent was obtained from the patients. The study was approved by the institutional review board of the Japanese Foundation for Cancer Research.

Immunohistochemistry

Formalin-fixed, paraffin-embedded tissue was sliced at a thickness of 4 μm, and the sections were placed on silane-coated slides. For antigen retrieval, the slides were heated for 45 minutes at 102°C in antigen retrieval solution (Nichirei Bioscience, Tokyo). For conventional immunostaining, the slides were incubated at room temperature with primary antibodies: ALK (5A4), vimentin, epithelial membrane antigen (EMA), cytokeratin 7, AE1/AE3, CAM5.2, 34βE12, α-methylacyl-coenzymeA racemase (AMACR), clusters of differentiation 10 (CD10), transcription termination factor 1 (TTF1), renal cell carcinoma marker (RCC Ma), paired box 2 (PAX2), and paired box 8 (PAX8) for 30 minutes. The immune complexes were then detected with polymer reagent (Histofine Simple Stain MAX PO; Nichirei Bioscience, Tokyo, Japan). For the sensitive detection of ALK fusion proteins, the ALK Detection Kit (Nichirei Bioscience), which is based on the iAEP method, was used.

Isolation of ALK Fusions

To obtain complementary DNA (cDNA) fragments corresponding to a novel ALK fusion gene, we used a 5′ rapid amplification of cDNA ends (5′-RACE) method with the SMARTer RACE cDNA Amplification Kit (Clontech, Takara Bio Inc., Shiga, Japan). We followed the manufacturer's instructions, with a minor modification: the ALK2458R primer (5′-GTAGTTGGGGTTGTAGTC GGTCATGATGGT-3′) was used as the gene-specific reverse primer. From the deoxythymidine oligomer–primed cDNA obtained from RNA from case 1, a 385–base pair (bp) cDNA fragment containing the fusion point was specifically amplified with the primers TPM3-705F (5′-AGAGACCCGTGCTGAGTTTGCTG-3′) and ALK3078RR (5′-ATCCAGTTCGTCCTGTTCA GAGC-3′). From case 2, a 454-bp cDNA fragment containing the fusion point was specifically amplified with the primers EML4-72F (5′-GTCAGCTCTTGAGT CACGAGTT-3′) and ALK3078RR. Polymerase chain reaction (PCR) analysis of genomic DNA for TPM3-ALK in case 1 was carried out with a pair of primers flanking the putative fusion point: TPM3-705F (5′-AGA GACCCGTGCTGAGTTTGCTG-3′) and Fusion-RT-AS (5′-TCTTGCCAGCAAAGCAGTAGTTGG-3′). For genomic PCR analysis of EML4-ALK in case 2, we used primers EML4-107F (5′-ATGAAATCACTGTGCTAA AGGCGGCT-3′) and Fusion-RT-AS (5′-TCTTGCCA GCAAAGCAGTAGTTGG-3′).

Fluorescence In Situ Hybridization

Fluorescence in situ hybridization (FISH) analysis of gene fusion was carried out with DNA probes for ALK, TPM3, EML4, and transcription factor E3 (TFE3). Unstained sections (4 μm thick) were subjected to hybridization with an ALK-split probe set (Dako, Tokyo, Japan), TFE3-split probe set (Kreatech, Amsterdam, The Netherlands), or bacterial artificial chromosome (BAC) clone-derived

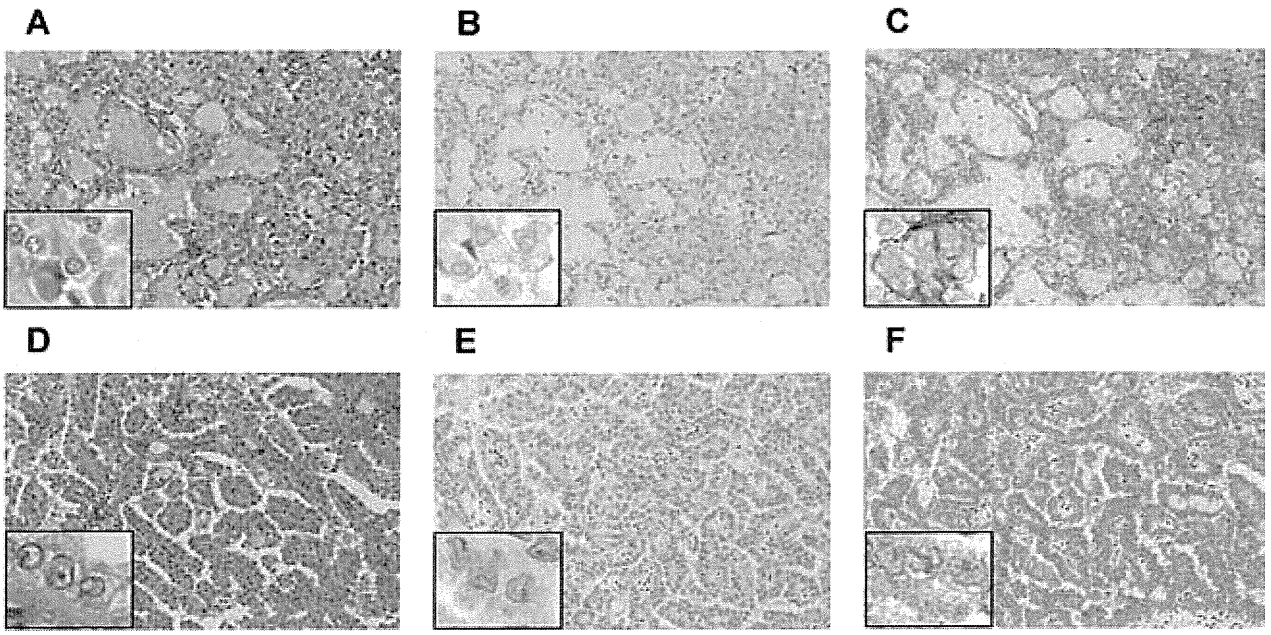

Figure 2. Histopathology of anaplastic lymphoma kinase (ALK)-positive renal cancer. Cuboidal tumor cells showed papillary, tubular, or cribriform growth patterns. The tumor cells had eosinophilic cytoplasm and round to ovoid nuclei. (A) The glandular structures possessed abundant mucin. (D) The tumor comprised a papillary structure of cuboidal or low columnar cells, with eosinophilic cytoplasm and small uniform round to oval nuclei (A,D hematoxylin and eosin stain). The tumor cells were (B) weakly positive and (E) indeterminate for ALK with conventional anti-ALK immunohistochemistry. (C,F) All of the tumor cells were clearly positive for ALK when the iAEP method was used. The staining pattern was diffuse cytoplasmic, with (C) membranous or (F) fine granular accentuation. Figures were taken using the corresponding whole sections (× 10 objective for low power view. × 40 objective for inset). Case 1 (A-C); Case 2 (D-F).

probes for ALK (RP11-984I21, RP11-62B19, RP11-701P18), TPM3 (RP11-809B24), and EML4 (RP11-996L7). Hybridized slides were then stained with 4′,6-diamidino-2-phenylindole and examined using a fluorescence microscope BX51 (Olympus, Tokyo, Japan).

Mutation Analyses for MET

A 1007-bp cDNA fragment containing the MET kinase domain was amplified using the primers MET-3186F (5′-GTCCATTACTGCAAAATACTGTCC-3′) and MET-4193R (5′-CACCTCATCATCAGCGTTATC-3′). The PCR product was sequenced after subcloning.

RESULTS

Identification of ALK Fusions in RCC Samples

Sections of tissue microarray were immunostained for ALK by the iAEP method, resulting in the detection of 2 positive cases (case 1, Fig. 2A-C; case 2, Fig. 2D-F). The positive results were also confirmed using corresponding whole histopathological sections, in which all of the tumor cells stained for ALK as other ALK-positive cancers usually do. We carried out 5′-RACE assays to determine whether these cases expressed ALK fusion or full-length ALK (mutated or unmutated). We isolated a cDNA fragment containing the exon 8 of *TPM3* fused in-frame to the exon 20 of *ALK* (Fig. 3A) in case 1, and the exon 2 of *EML4* fused to the exon 20 of *ALK* in case 2 (Fig. 3B). This EML4-ALK is called variant 5 (E2;A20) in lung cancer.[30] Reverse transcription PCR (RT-PCR) assays designed for the *TPM3-ALK* or E2;A20 successfully amplified cDNAs containing the fusion points (Fig. 3C,D). To confirm the genomic rearrangement, we performed FISH assays (Fig. 4) and genomic PCR (data not shown) for each fusion. All our results were consistent with the presence of t(1;2)(p21;p23)/*TPM3-ALK* in case 1, or inv(2)(p21p23)/E2;A20 in case 2. No other cases were positive for ALK by iAEP immunohistochemistry. All 355 cases were further examined by ALK-split FISH assay. In 12 of the cases, FISH was unsuccessful and not evaluable. In the other cases, the results were identical to those obtained by anti-ALK iAEP immunohistochemistry.

Case Presentation

Case 1

The patient was a 36-year-old woman who had a complaint suggestive of pyelonephritis. Magnetic resonance imaging and computed tomography showed a mass (4.0 cm × 4.0 cm × 3.5 cm) in the left kidney. No metastatic lesions or lymph node enlargements were identified. The patient had no past medical history of malignancy.

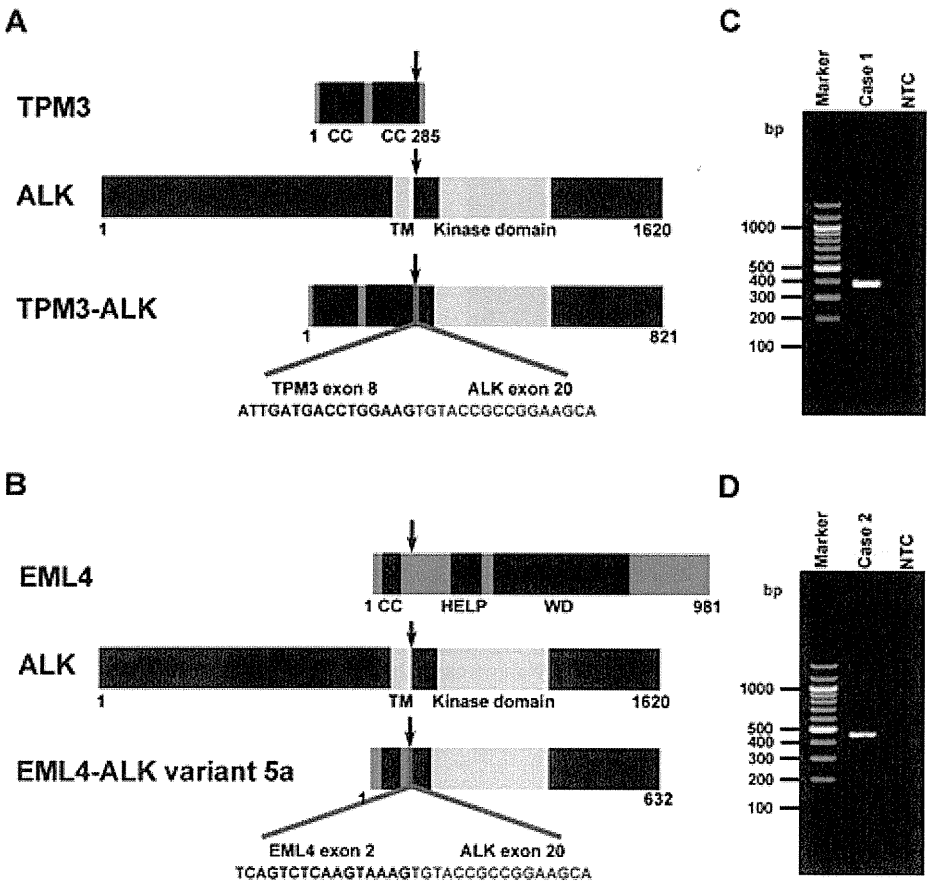

Figure 3. Identification of anaplastic lymphoma kinase (ALK) fusions. Tropomyosin 3 (TPM3) harbors 2 coiled-coil domains. (A) Case 1. A chromosome translocation generates a fusion protein in which the 2 coiled-coil domains of TPM3 and the intracellular region of ALK (containing the tyrosine kinase domain) are conserved. (B) Nucleotide sequencing of the polymerase chain reaction (PCR) products in case 2 revealed that exon 2 of echinoderm microtubule-associated protein like 4 (EML4), comprising a coiled-coil domain, was fused to exon 20 of ALK, generating the variant 5 complementary DNA (cDNA). In TPM3 and EML4 fusions, the region containing the coiled-coil domain is fused to the kinase domain of ALK. Numbers indicate amino acid positions of each protein. Arrow indicates the chromosomal breakpoint. The cDNA fragments of 385 base pairs (bp) and 454 bp were obtained by reverse transcription PCR, corresponding to (C) *TPM3-ALK* and (D) *EML4-ALK* variant 5, respectively. The left lane ("Marker") contains DNA size standards (100-bp ladder). CC indicates coiled-coil domain; HELP, hydrophobic echinoderm microtubule-associated protein; NTC, no-template control; TM, transmembrane domain; WD, WD repeats.

She underwent a translumbar left-radical nephrectomy and is currently alive and well without evidence of disease at 2 years of follow-up.

Case 2

A 53-year-old woman was found incidentally to have microscopic hematuria by medical check-up. Ultrasonography and magnetic resonance imaging showed a change in the left kidney, but the diagnosis was indefinite at that time. One year later, adenocarcinoma cells were detected by urinary cytology, and computed tomography revealed an isodence left renal mass (2.5 cm × 2.5 cm × 2.3 cm). The patient underwent a translumbar left-radical nephrectomy. She is currently alive and well at 7 years after surgery.

The patients had no episodes or family history indicative of sickle cell trait. To the best of our knowledge, there is no reported case of (genetically) Japanese individuals with sickle cell trait/disease.

Histopathological Examinations

The 2 ALK-positive renal cancers were papillary subtype and unclassified (with mixed features of papillary, mucinous cribriform, and solid patterns with rhabdoid cells). They comprised 2.3% of non–clear cell RCCs (2 of 88) and 3.7% of non–clear cell and nonchromophobe RCCs (2 of 54).

Case 1

Histologically, tumor cells were composed of papillary, tubular, or cribriform growth of cuboidal cells with

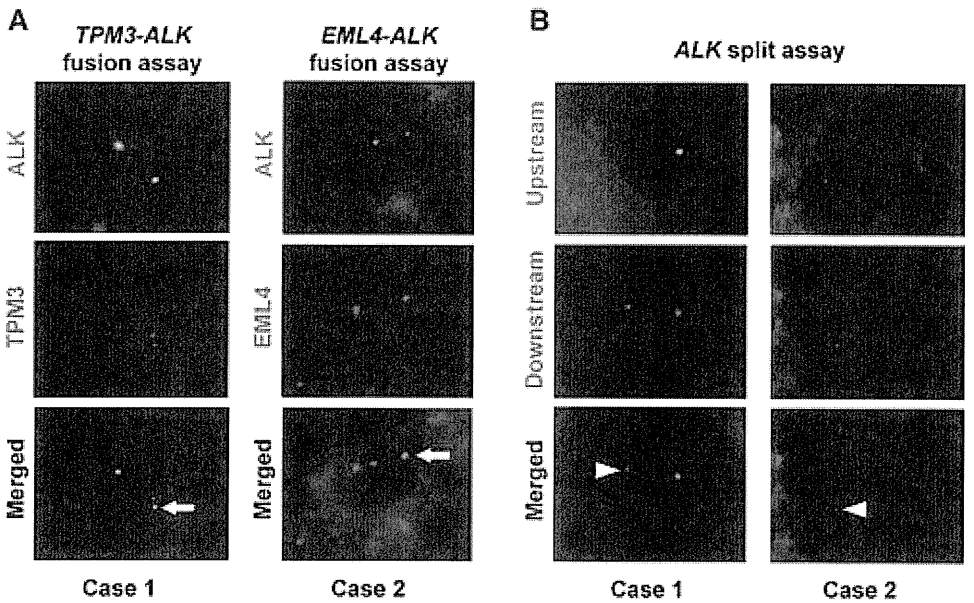

Figure 4. Fluorescence in situ hybridization analyses for *TPM3-ALK* (tropomyosin 3 fusion with anaplastic lymphoma kinase) and *EML4-ALK* (echinoderm microtubule-associated protein like 4 fusion with ALK). (A) In the *TPM3-ALK* and *EML4-ALK* fusion assays, the fusion genes are indicated by arrows. (B) The same clinical specimens as in (A) were subjected to fluorescence in situ hybridization analysis with differentially labeled probes for the upstream (green) or downstream (red) to the ALK breakpoint. In each case, the absence of 1 upstream signal indicated ALK rearrangement. Arrowhead indicates the rearranged ALK. The color of fluorescence for the bacterial artificial chromosome clones and the case numbers are indicated. Nuclei are stained blue with 4′,6-diamidino-2-phenylindole.

eosinophilic cytoplasm. The cribriform morphology consisted of tubular structures with flattened epithelial cells, compressed by mucinous pool and inter- or intracytoplasmic vacuoles. Solid sheets of tumor cells with occasional deeply eosinophilic intracytoplasmic inclusions and eccentric nuclei, resulting in rhabdoid features, were focally identified. Nuclei were round to ovoid, and the nuclear size was basically uniform. Irregular nuclear membranes and nuclear grooves were occasionally observed. Mitotic figures were scant. The background stroma in the tumor area possessed abundant mucin. Frequent deposition of psammoma bodies and infiltration of numerous foamy macrophages were also seen. A large amount of mucinous matrix was highlighted with Alcian blue stain. These histological features resembled the mucinous cribriform pattern frequently observed in ALK-positive lung adenocarcinoma,[18,31] and also a representative case of unclassified RCC by Lopez-Beltran et al,[32] favoring a diagnosis of unclassified RCC. Immunohistochemically, neoplastic cells showed a diffuse and strong positivity for ALK (iAEP), vimentin, EMA, cytokeratin 7, AE1/AE3, cytokeratin CAM5.2, and cytokeratin 34βE12, and focally staining for PAX2, PAX8, AMACR, and CD10. TTF1 and RCC Ma were completely negative. Intracytoplasmic inclusions corresponded to aggregates of intermediate filaments of vimentin. The ALK-staining pattern appeared to be accentuated around the cell membrane of rhabdoid cells. The MIB1 (mindbomb homolog 1) labeling index was less than 1%.

Case 2

Histologically, the tumor consisted of papillary configuration of cuboidal or low columnar cells, with eosinophilic cytoplasm and small uniform round to oval nuclei. A clear cell change was focally seen. Nuclei showed a round to oval shape, and nuclear grooves were frequently observed. The size variation of nuclei was minimal, and the irregularity of the nuclear membrane was evident. Nuclear pseudoinclusions were seldom seen. Small nucleoli were occasionally identified, but mitoses were absent. The fibrovascular cores of papillary architecture contained numerous psammoma bodies and foamy macrophages. In addition, glandular lumens of tumor cells focally contained myxoid materials. These findings morphologically corresponded to papillary RCC, but did not fit to types 1 and 2 by the classification of Delahunt and Eble.[33] In contrast, the features resembled papillary RCC, type 2A, described by Yang et al.[34] Alcian blue stain highlighted a small amount of stromal-type mucin. Upon immunohistochemical analysis, neoplastic cells were diffusely and

strongly positive for ALK (iAEP), vimentin, EMA, cytokeratin 7, AE1/AE3, cytokeratin CAM5.2, cytokeratin 34βE12, and AMACR, and focally positive for PAX2 and PAX8, but negative for TTF1, CD10, and RCC Ma.

Examinations of Other Gene Aberrations

For *MET*, a cDNA fragment with the predicted size was obtained by RT-PCR in case 1. In case 2, no products were identified, indicating that the tumor of the patient did not express *MET*. No mutations were identified in case 1 by sequencing. TFE3 split signals were not observed in either of the 2 cases by FISH.

DISCUSSION

Recently, 2 independent groups have reported vinculin-ALK (VCL-ALK) in renal cancer (Table 1).[35,36] These findings broaden the spectrum of ALK fusion–positive tumors. Interestingly, the 2 patients described in the reports share several uncommon backgrounds for renal cancer: very early onset (6- and 16-year-old boys), a history of sickle cell trait, and uncommon histopathological subtypes (medullary subtype and indeterminate subtype with mixed features of medullary, chromophobe, and transitional cell subtypes). In this study, we screened 355 renal tumors, including 343 RCCs, and identified ALK fusions in 2 RCCs. Significantly, we identified ALK fusions in adult patients (36- and 53-year-old females) without sickle cell trait. This finding will provide a key to ALK inhibitor therapy for more common renal cancers.

RCC associated with *TFE3* gene fusions is already a distinctive entity in the World Health Organization classification,[37,38] and *MET* mutation has been described in 13% of sporadic papillary RCCs.[39] In the present study, we identified neither *MET* nor *TFE3* aberrations in our ALK-positive renal cancer cases. *ALK* rearrangements are recognized as almost mutually exclusive to other mutations such as *EGFR* (epidermal growth factor receptor) and *KRAS* (v-Ki-ras2 Kirsten rat sarcoma viral oncogene) in lung cancer.[6,40] All of the tumor cells in the 2 ALK-positive renal cancers observed by immunohistochemistry expressed ALK fusion protein, suggesting that all tumor cells harbor one or more *ALK* fusion genes. Therefore, as well as other ALK-positive tumors, *ALK* rearrangement in renal cancer probably occurs at a very early phase of carcinogenesis, and is likely to be a driver mutation and mutually exclusive to other driver mutations. As in the case of ALK-positive ALCL, ALK-positive renal cancer will be a distinct molecular pathological entity.

TPM3-ALK was first identified in ALCL in 1999,[41] and subsequently found in IMT in 2000.[5] Therefore, RCC is the third type of cancer that may harbor TPM3-ALK. The organ distribution of EML4-ALK is somewhat controversial. Since its discovery, EML4-ALK has been reported to be identified in lung, breast, and colon cancers. Many research groups have reported the presence of EML4-ALK in a small subset of lung adenocarcinomas (2%-10%). Interestingly, a group in the United States reported the presence of EML4-ALK in breast (5 of 209) and colorectal (2 of 83) cancers, identified by RT-PCR optimized for variants 1, 2, and 3, without showing histopathological evidence.[42] In contrast, 2 Japanese groups examined these cancers (90 breast and 96 colon cancers by RT-PCR for EML4-ALK variants 1 and 2, and 48 breast and 50 colon cancers by multiplex RT-PCR for all possible fusions), but detected no positive cases.[30,43] One possible reason for this discrepancy may be differences in ethnicity. In the present study, we showed histopathological features of the 2 ALK-positive renal cancers. In addition to morphology, the positivity of PAX2 and PAX8 and the negativity of TTF1 strongly indicated that the ALK-positive cancers of the present cases were primary RCCs, and not metastatic lesions of ALK-positive lung cancer.

The oncogenic activities of TPM3-ALK and EML4-ALK have previously been documented,[30,44] and therefore we did not demonstrate them in the present study. As in the case of other ALK-positive tumors, ALK-positive renal cancer is a promising candidate disease for ALK inhibitor therapy. In the present study, we screened surgically removable cases; the prognoses for the 2 ALK-positive patients were good, without recurrence. To realize the full potential of ALK inhibitors in renal cancers, it is important to identify the detailed clinicopathological features of ALK-positive cases, especially those of advanced or recurrent cases, by large-scale screening. For this purpose, anti-ALK immunohistochemistry can most readily be carried out as a primary screening tool. However, caution is needed; the screening immunohistochemical assay should be appropriately sensitive, because our present findings indicate that renal cancer involves EML4-ALK, which is barely detectable by conventional immunohistochemistry methods.[13,45]

Is morphology a clue to the presence of ALK fusion in renal cancers? Almost all ALK-positive lung cancers are adenocarcinomas, and more frequently show mucinous cribriform patterns and signet-ring cells than do ALK-negative adenocarcinomas.[18,31,46] ALK fusion is probably very rare in clear cell RCC, which is the most common

Table 1. ALK-Positive Renal Cancers: Present Cases and Review of Literature

Characteristic	VCL-ALK (Debelenko et al[36])	VCL-ALK (Marino-Enriquez et al[35])	TPM3-ALK (Case 1)	EML4-ALK (Case 2)
Age, y	16	6	36	53
Sex	Male	Male	Female	Female
Ethnicity	African American	African American	Japanese	Japanese
Past history	Sickle cell trait	Sickle cell trait	Tuberculosis (22 y old)	Pleomorphic adenoma (50 y old)
Karyotype	Abnormal complex karyotype	46,XY,t(2;10)(p23;q22), add(14)(p11)	Not examined	Not examined
Symptom	Right flank pain, gross hematuria	Intermittent periumbilical pain, hematuria	Pyelonephritis	Microscopic hematuria
Stage	Stage III	Stage I	Stage I	Stage I
Follow-up	9 mo, alive. No evidence of disease	21 mo, alive. No evidence of disease	2 y, alive. No evidence of disease	3 y, alive. No evidence of disease
Gross findings	6.5-cm irregularly shaped solid tumor mass with infiltrative borders centered in the right renal medulla	4.5-cm irregularly spherical mass with lobulated, fleshy light tan appearance centered in the medulla	4.0 cm × 4.0 cm × 3.5 cm irregularly shaped solid tumor with expansive borders centered in the cortex	Double cancer. A: 2.5 cm × 2.5 cm ×2.3 cm solid yellow tumor in the cortex of the left intermediate pole. B: 0.6-cm yellow mass in the cortex of the left inferior pole
Microscopic findings	Diffuse sheet-like pattern; round, oval, and polygonal tumor cells; eosinophilic cytoplasm; moderately polymorphic and vesicular nuclei	Solid growth pattern; spindle-shaped cells with large vesicular nuclei; clear coarse chromatin and abundant eosinophilic cytoplasm	Papillary, tubular, or cribriform growth of cuboidal cells with eosinophilic cytoplasm. Nuclei round to ovoid; nuclear size basically uniform	A: Papillary structure of cuboidal or low columnar cells with eosinophilic cytoplasm and small uniform round to oval nuclei. B: Clear cell
Immunohistochemistry	Positive: AE1/AE3, CAM5.2, CK7, EMA, INI1, TFE3. Negative: CD10, S100, HMB45, WT1	Positive: AE1/AE3, CAM5.2, EMA	Positive: ALK, vimentin, EMA, cytokeratin 7, AE1/AE3, CAM5.2, 34βE12, AMACR (focal), CD10 (focal), PAX2 (focal), PAX8 (focal). Negative: TTF1, RCC Ma	A: Positive: ALK, vimentin, EMA, cytokeratin 7, AE1/AE3, CAM5.2, 34βE12, AMACR, PAX2 (focal), PAX8 (focal). Negative: CD10, TTF1, RCC Ma
Diagnosis	Renal cell carcinoma, indeterminate subtype (medullary, chromophobe, transitional cell carcinoma mixed)	Renal medullary carcinoma	Renal cell carcinoma, unclassified	A: Papillary renal cell carcinoma, type 2A. B: Clear cell renal cell carcinoma

ALK indicates anaplastic lymphoma kinase; EML4, echinoderm microtubule–associated protein like 4; TPM3, tropomyosin 3; VCL, vinculin.

subtype of renal cancer; 2 previously reported cases with VCL-ALK were not clear cell RCC,[35,36] and we identified no ALK-positive cases in 255 clear cell RCCs in this study. Interestingly, case 1 showed a mucinous cribriform pattern. This may be a characteristic feature of ALK-positive carcinomas, universally applicable to carcinomas of various organs. Further study with a larger number of cases is warranted.

Molecular-targeted therapy of advanced renal cancers is starting to realize its full potential. However, complete remission is rarely achieved, because no agent targets a key molecule associated with "oncogene addiction" of renal cancer. In this context, ALK fusion constitutes a promising advance in renal cancers, as has previously been demonstrated with various other types of cancer. In the present study, we identified 2 adult cases of ALK-positive renal cancer in patients without uncommon backgrounds. Our findings confirm the potential of ALK inhibitor therapy for RCC. More detailed clinicopathological features of ALK-positive renal cancers, especially at higher clinical stages, are desirable. Hunting the "ALKoma" in various types of carcinomas, as well as in lung and kidney cancer, will provide an answer to these pathological and clinical questions.

FUNDING SOURCES

This work was supported in part by Grants-in-Aid for Scientific Research from the Ministry of Education, Culture, Sports, Science, and Technology of Japan as well as by grants from the Japan Society for the Promotion of Science; the Ministry of Health, Labour, and Welfare of Japan; the Vehicle Racing Commemorative Foundation of Japan; Princess Takamatsu Cancer Research Fund; and the Uehara Memorial Foundation.

CONFLICT OF INTEREST DISCLOSURE

Dr. Takeuchi is a scientific advisor for the anti-ALK iAEP immunohistochemistry kit (ALK Detection Kit, Nichirei Bioscience, Tokyo, Japan). All remaining authors have made no disclosures.

REFERENCES

1. International Agency for Research on Cancer. The GLOBOCAN Project: GLOBOCAN 2008. http://globocan.iarc.fr/. Accessed December 16, 2011.
2. Campbell SC, Novick AC, Bukowski RM. Renal tumors. In: Wein AJ, Kavoussi LR, Novick AC, Partin AW, Peters CA, eds. Campbell-Walsh Urology. 9th ed. Philadelphia, PA: Saunders; 2007: 1567-1637.
3. Morris SW, Kirstein MN, Valentine MB, et al. Fusion of a kinase gene, ALK, to a nucleolar protein gene, NPM, in non-Hodgkin's lymphoma. *Science.* 1994;263:1281-1284.
4. Shiota M, Fujimoto J, Semba T, Satoh H, Yamamoto T, Mori S. Hyperphosphorylation of a novel 80 kDa protein-tyrosine kinase similar to Ltk in a human Ki-1 lymphoma cell line, AMS3. *Oncogene.* 1994;9:1567-1574.
5. Lawrence B, Perez-Atayde A, Hibbard MK, et al. TPM3-ALK and TPM4-ALK oncogenes in inflammatory myofibroblastic tumors. *Am J Pathol.* 2000;157:377-384.
6. Soda M, Choi YL, Enomoto M, et al. Identification of the transforming EML4-ALK fusion gene in non-small-cell lung cancer. *Nature.* 2007;448:561-566.
7. Rikova K, Guo A, Zeng Q, et al. Global survey of phosphotyrosine signaling identifies oncogenic kinases in lung cancer. *Cell.* 2007; 131:1190-1203.
8. Soda M, Takada S, Takeuchi K, et al. A mouse model for EML4-ALK-positive lung cancer. *Proc Natl Acad Sci U S A.* 2008;105: 19893-19897.
9. Kwak EL, Bang YJ, Camidge DR, et al. Anaplastic lymphoma kinase inhibition in non-small-cell lung cancer. *N Engl J Med.* 2010;363:1693-1703.
10. Chihara D, Suzuki R. More on crizotinib. *N Engl J Med.* 2011;364: 776-777.
11. Butrynski JE, D'Adamo DR, Hornick JL, et al. Crizotinib in ALK-rearranged inflammatory myofibroblastic tumor. *N Engl J Med.* 2010;363:1727-1733.
12. Gambacorti-Passerini C, Messa C, Pogliani EM. Crizotinib in anaplastic large-cell lymphoma. *N Engl J Med.* 2011;364:775-776.
13. Takeuchi K, Choi YL, Togashi Y, et al. KIF5B-ALK, a novel fusion oncokinase identified by an immunohistochemistry-based diagnostic system for ALK-positive lung cancer. *Clin Cancer Res.* 2009;15: 3143-3149.
14. Martelli MP, Sozzi G, Hernandez L, et al. EML4-ALK rearrangement in non-small cell lung cancer and non-tumor lung tissues. *Am J Pathol.* 2009;174:661-670.
15. Jokoji R, Yamasaki T, Minami S, et al. Combination of morphological feature analysis and immunohistochemistry is useful for screening of EML4-ALK-positive lung adenocarcinoma. *J Clin Pathol.* 2010;63:1066-1070.
16. Kijima T, Takeuchi K, Tetsumoto S, et al. Favorable response to crizotinib in three patients with echinoderm microtubule-associated protein-like 4-anaplastic lymphoma kinase fusion-type oncogene-positive non-small cell lung cancer. *Cancer Sci.* 2011;102:1602-1604.
17. Kimura H, Nakajima T, Takeuchi K, et al. ALK fusion gene positive lung cancer and 3 cases treated with an inhibitor for ALK kinase activity. *Lung Cancer.* 2012;75:66-72.
18. Yoshida A, Tsuta K, Nakamura H, et al. Comprehensive histologic analysis of ALK-rearranged lung carcinomas. *Am J Surg Pathol.* 2011;35:1226-1234.
19. Yi ES, Boland JM, Maleszewski JJ, et al. Correlation of IHC and FISH for ALK gene rearrangement in non-small cell lung carcinoma: IHC score algorithm for FISH. *J Thorac Oncol.* 2011;6:459-465.
20. Kudo K, Takeuchi K, Tanaka H, et al. Immunohistochemical screening of ALK lung cancer with biopsy specimens of advanced lung cancer. *J Clin Oncol.* 2010;28(suppl): (abstract 10532).
21. Sakairi Y, Nakajima T, Yasufuku K, et al. EML4-ALK fusion gene assessment using metastatic lymph node samples obtained by endobronchial ultrasound-guided transbronchial needle aspiration. *Clin Cancer Res.* 2010;16:4938-4945.
22. Nakajima T, Kimura H, Takeuchi K, et al. Treatment of lung cancer with an ALK Inhibitor after EML4-ALK fusion gene detection using endobronchial ultrasound-guided transbronchial needle aspiration. *J Thorac Oncol.* 2010;5:2041-2043.
23. Takeuchi K, Soda M, Togashi Y, et al. Identification of a novel fusion, SQSTM1-ALK, in ALK-positive large B-cell lymphoma. *Haematologica.* 2011;96:464-467.
24. Takeuchi K, Soda M, Togashi Y, et al. Pulmonary inflammatory myofibroblastic tumor expressing a novel fusion, PPFIBP1-ALK: reappraisal of anti-ALK immunohistochemistry as a tool for novel ALK-fusion identification. *Clin Cancer Res.* 2011;17:3341-3348.
25. Shiota M, Fujimoto J, Takenaga M, et al. Diagnosis of t(2;5)(p23;q35)-associated Ki-1 lymphoma with immunohistochemistry. *Blood.* 1994;84:3648-3652.
26. Pulford K, Lamant L, Morris SW, et al. Detection of anaplastic lymphoma kinase (ALK) and nucleolar protein nucleophosmin (NPM)-ALK proteins in normal and neoplastic cells with the monoclonal antibody ALK1. *Blood.* 1997;89:1394-1404.
27. Shiota M, Nakamura S, Ichinohasama R, et al. Anaplastic large cell lymphomas expressing the novel chimeric protein p80NPM/ALK: a distinct clinicopathologic entity. *Blood.* 1995;86:1954-1960.
28. Delsol G, Lamant L, Mariamé B, et al. A new subtype of large B-cell lymphoma expressing the ALK kinase and lacking the 2; 5 translocation. *Blood.* 1997;89:1483-1490.
29. Lamant L, Pulford K, Bischof D, et al. Expression of the ALK tyrosine kinase gene in neuroblastoma. *Am J Pathol.* 2000;156:1711-1721.
30. Takeuchi K, Choi YL, Soda M, et al. Multiplex reverse transcription-PCR screening for EML4-ALK fusion transcripts. *Clin Cancer Res.* 2008;14:6618-6624.
31. Inamura K, Takeuchi K, Togashi Y, et al. EML4-ALK fusion is linked to histological characteristics in a subset of lung cancers. *J Thorac Oncol.* 2008;3:13-17.
32. Lopez-Beltran A, Carrasco JC, Cheng L, Scarpelli M, Kirkali Z, Montironi R. 2009 update on the classification of renal epithelial tumors in adults. *Int J Urol.* 2009;16:432–443.
33. Delahunt B, Eble JN. Papillary renal cell carcinoma: a clinicopathologic and immunohistochemical study of 105 tumors. *Mod Pathol.* 1997;10:537-544.
34. Yang XJ, Tan MH, Kim HL, et al. A molecular classification of papillary renal cell carcinoma. *Cancer Res.* 2005;65:5628-5637.
35. Mariño-Enríquez A, Ou WB, Weldon CB, Fletcher JA, Pérez-Atayde AR. ALK rearrangement in sickle cell trait-associated renal medullary carcinoma. *Genes Chromosomes Cancer.* 2011;50:146-153.
36. Debelenko LV, Raimondi SC, Daw N, et al. Renal cell carcinoma with novel VCL-ALK fusion: new representative of ALK-associated tumor spectrum. *Mod Pathol.* 2011;24:430-442.
37. Argani P, Ladanyi M. Renal carcinomas associated with Xp11.2 translocations/TFE3 gene fusions. In: Eble J, Sauter G, Epstein J, Sesterhenn I, eds. Pathology and Genetics of Tumours of the Urinary System and Male Genital Organs. Lyon, France: IARC Press; 2004:37-38.
38. Ross H, Argani P. Xp11 translocation renal cell carcinoma. *Pathology.* 2010;42:369-373.

39. Schmidt L, Junker K, Nakaigawa N, et al. Novel mutations of the MET proto-oncogene in papillary renal carcinomas. *Oncogene.* 1999; 18:2343-2350.
40. Inamura K, Takeuchi K, Togashi Y, et al. EML4-ALK lung cancers are characterized by rare other mutations, a TTF-1 cell lineage, an acinar histology, and young onset. *Mod Pathol.* 2009;22:508-515.
41. Lamant L, Dastugue N, Pulford K, Delsol G, Mariamé B. A new fusion gene TPM3-ALK in anaplastic large cell lymphoma created by a (1;2)(q25;p23) translocation. *Blood.* 1999;93: 3088-3095.
42. Lin E, Li L, Guan Y, et al. Exon array profiling detects EML4-ALK fusion in breast, colorectal, and non-small cell lung cancers. *Mol Cancer Res.* 2009;7:1466-1476.
43. Fukuyoshi Y, Inoue H, Kita Y, Utsunomiya T, Ishida T, Mori M. EML4-ALK fusion transcript is not found in gastrointestinal and breast cancers. *Br J Cancer.* 2008;98:1536-1539.
44. Giuriato S, Faumont N, Bousquet E, et al. Development of a conditional bioluminescent transplant model for TPM3-ALK-induced tumorigenesis as a tool to validate ALK-dependent cancer targeted therapy. *Cancer Biol Ther.* 2007;6:1318-1323.
45. Sozzi G, Martelli MP, Conte D, et al. The EML4-ALK transcript but not the fusion protein can be expressed in reactive and neoplastic lymphoid tissues. *Haematologica.* 2009;94:1307-1311.
46. Rodig SJ, Mino-Kenudson M, Dacic S, et al. Unique clinicopathologic features characterize ALK-rearranged lung adenocarcinoma in the western population. *Clin Cancer Res.* 2009;15:5216-5223.

Cancer Science
The official journal of the Japanese Cancer Association JCA

Case Report

Favorable response to crizotinib in three patients with echinoderm microtubule-associated protein-like 4–anaplastic lymphoma kinase fusion-type oncogene-positive non-small cell lung cancer

Takashi Kijima,[1,3] Kengo Takeuchi,[2] Satoshi Tetsumoto,[1] Kazuki Shimada,[1] Ryo Takahashi,[1] Haruhiko Hirata,[1] Izumi Nagatomo,[1] Shigenori Hoshino,[1] Yoshito Takeda,[1] Hiroshi Kida,[1] Sho Goya,[1] Isao Tachibana[1] and Ichiro Kawase[1]

[1]Department of Respiratory Medicine, Allergy and Rheumatic Diseases, Osaka University Graduate School of Medicine, Osaka; [2]Pathology Project for Molecular Targets, Cancer Institute, Japanese Foundation for Cancer Research, Tokyo, Japan

(Received March 7, 2011/Revised April 21, 2011/Accepted April 21, 2011)

The echinoderm microtubule-associated protein-like 4 (EML4)–anaplastic lymphoma kinase (ALK) is a recently identified fusion-type oncoprotein that exists in approximately 5% of non-small cell lung cancer (NSCLC). It has been demonstrated that NSCLC driven by EML4-ALK is strongly addicted to this fusion-type oncokinase. A clinical trial of crizotinib (PF-02341066) sponsored by Pfizer has proven this oncogene addiction in humans by demonstrating a high response rate to inhibition of ALK kinase activity. In the present study, we report on three cases harboring *EML4-ALK* rearrangement who were enrolled in the trial (A8081001, NCT00585195). All three patients showed favorable responses to the ALK-specific tyrosine kinase inhibitor. (*Cancer Sci* 2011; 102: 1602–1604)

Case report

Clinical findings in three patients treated with crizotinib are described below.

Case 1. A 30-year-old man who had never smoked presented with smoldering pneumonia in October 2008. A diagnosis of Stage IIIB (cT2N3M0) lung adenocarcinoma was made and the patient subsequently received two cycles of systemic chemotherapy with cisplatin and vindesine, with concurrent thoracic irradiation, followed by two cycles of consolidation with carboplatin and paclitaxel. This treatment regimen resulted in stable disease. The primary tumor did not have epidermal growth factor receptor (*EGFR*) mutations, but immunohistochemistry (IHC) was positive for anaplastic lymphoma kinase (ALK) protein using the intercalated antibody-enhanced polymer (iAEP) method with 5A4 (Abcam, Cambridge, UK) as the primary antibody (Fig. 1a).[1] Fluorescence *in situ* hybridization (FISH), using probes described elsewhere,[2] confirmed echinoderm microtubule-associated protein-like 4 (*EML4*)–*ALK* rearrangement (Fig. 1b). Multiplex RT-PCR[1,3] further showed that this patient's fusion type was variant 3 (Fig. 1c). The patient was enrolled in the trial in April 2009.[4] The patient's persistent cough disappeared within 2 weeks of initiation of oral crizotinib therapy (250 mg twice daily) and the primary tumor shrank. Although there was no change in the size of the mediastinal lymph nodes, PET CT demonstrated marked reductions in the accumulation of fluorodeoxyglucose (^{18}F) after 12 months (Fig. 1d). Transient mild nausea and diarrhea were observed for the first 4 weeks of treatment, but were well controlled over the subsequent 19 months without any other toxicity. Follow-up MRI of the brain in November 2010 showed the appearance of asymptomatic but multiple new lesions, despite favorable control outside the central nervous system (CNS). The patient received whole-brain radiotherapy in December 2010; thereafter, crizotinib was resumed after a 4-week break. The patient is currently continuing crizotinib treatment for 24 months in total.

Case 2. A 29-year-old man who was a heavy smoker presented with progressive lumbago in May 2009. Shortly thereafter, sudden onset symmetrical leg paralysis developed. Because MRI revealed tumors in multiple segments of the thoracic and lumbar spine, emergent radiotherapy to the 10th–12th thoracic vertebrae was performed. This patient's disease was diagnosed as Stage IV (cT2N3M1) lung adenocarcinoma with single brain and multiple bone metastases. Tests for *EGFR* mutations were negative and the patient was given two cycles of systemic chemotherapy with cisplatin and vinorelbine. After insertion of a cyber knife into the brain lesion, the patient was given a cycle of carboplatin and paclitaxel, resulting in stable disease. On the evidence of ALK-positive iAEP IHC (Fig. 2a) with confirmatory FISH-positive *EML4-ALK* rearrangement, oral crizotinib therapy (250 mg twice daily) was started in September 2009. All tumors except for the brain lesion shrank significantly and the patient was able to cease opioid within 1 month. Mild nausea, alternating diarrhea and constipation, and the persistence of light spectrum image bothered the patient for a few months and dysgeusia lasted throughout the duration of treatment, but these adverse events were not so severe as to diminish the patient's activities of daily living. After 6 months, a chest CT showed complete regression of the thoracic lesions and bone scintigraphy showed a marked reduction in the accumulation of ^{88m}Tc (Fig. 2b). The brain lesion remained stable and other pre-existing tumors disappeared for 9 months. However, multiple new lesions appeared in the liver and crizotinib therapy was therefore discontinued. Thereafter, the patient received four cycles of carboplatin, pemetrexed, and bevacizumab and is now being followed-up with the latter two agents being used as maintenance therapy.

Case 3. A 31-year-old man who was a light smoker presented with an asymptomatic abnormal shadow on chest X-ray found as part of the annual medical checkup in August

[3]To whom correspondence should be addressed.
E-mail: tkijima@imed3.med.osaka-u.ac.jp

doi: 10.1111/j.1349-7006.2011.01970.x

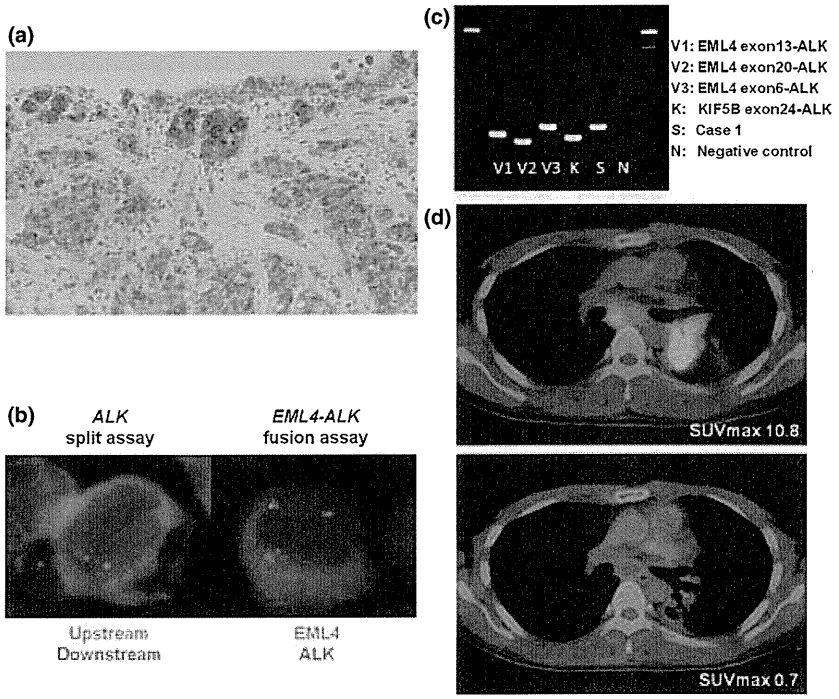

Fig. 1. (a) Intercalated antibody-enhanced polymer immunohistochemistry showing anaplastic lymphoma kinase (ALK) protein expression in acinar-type adenocarcinoma in Case 1. (b) Fluorescence *in situ* hybridization confirmed the *EML4-ALK* fusion gene. The ALK split assay was performed by labeling with probes for the upstream (green) and downstream (red) region of the *ALK* locus. The *EML4-ALK* fusion assay was performed by labeling with probes for *EML4* (green) and *ALK* (red). (c) Multiplex RT-PCR demonstrated the presence of *EML4-ALK* variant (V) 3. (d) Scans (PET CT) before (upper) and 12 months after (lower) crizotinib treatment. Accumulation of fluorodeoxyglucose (^{18}F) decreased markedly with maximum standardized uptake value (SUVmax) decreasing from 10.8 to 0.7. EML4, echinoderm microtubule-associated protein-like 4.

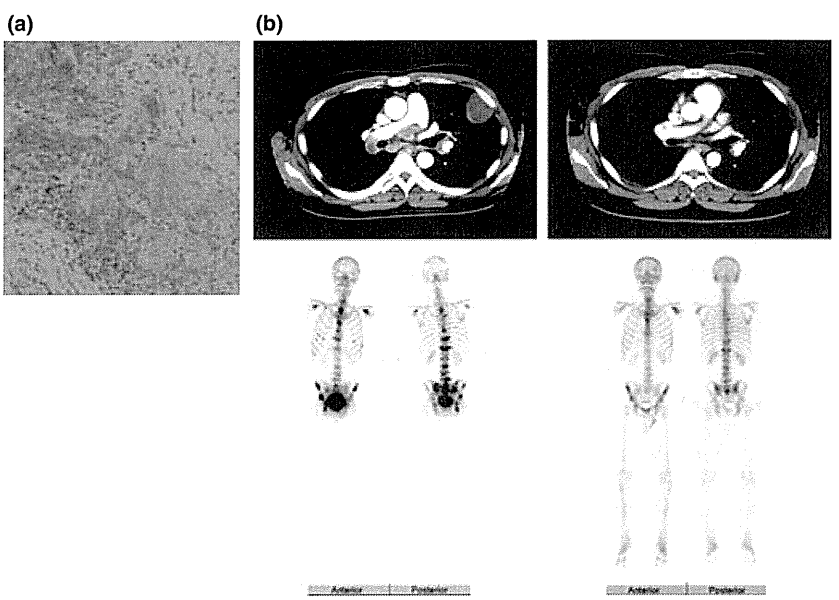

Fig. 2. (a) Intercalated antibody-enhanced polymer immunohistochemistry showing anaplastic lymphoma kinase protein expression in acinar-type adenocarcinoma in Case 2. (b) Chest CT and bone scintigraphy before (left) and 6 months after (right) crizotinib treatment. The tumors in the thorax almost disappeared and accumulation of ^{88m}Tc in multiple bones also decreased markedly.

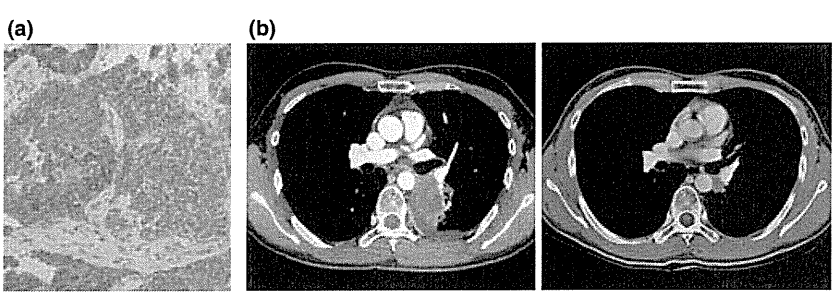

Fig. 3. (a) Intercalated antibody-enhanced polymer immunohistochemistry showing anaplastic lymphoma kinase protein expression in acinar-type adenocarcinoma in Case 3. (b) Chest CT before (left) and 12 months after (right) crizotinib treatment. Left pleural effusion disappeared and the primary tumor in the S6 segment shrank significantly.

2009. This patient's disease was diagnosed as Stage IIIB (cT4N0M0) lung adenocarcinoma with pleural dissemination. Chemoradiotherapy with cisplatin and vinorelbine failed after one cycle. Because tests for *EGFR* mutations were negative, but iAEP IHC (Fig. 3a) and FISH analyses revealed his tumor to be positive for *EML4-ALK*, the patient was started on oral crizotinib (250 mg twice daily) in December 2009. He achieved partial response shortly thereafter and the favorable

effect has lasted thus far for 17 months (Fig. 3b). The patient is currently continuing on crizotinib treatment. As for adverse effects, mild nausea and diarrhea were noted temporarily for the first 4 weeks of treatment, but persistence of vision spectrum and dysgeusia have lasted for the duration of the treatment period.

Discussion

The malignant transformation of approximately 5% of non-small cell lung cancer (NSCLC), especially adenocarcinoma, is caused by EML4-ALK and it is mutually exclusive for *EGFR* and *KRAS* mutations.[3,5–7] Basic research has shown that *EML4-ALK*-driven NSCLC is strongly addicted to this fusion-type oncogene.[5,8–10] Crizotinib is an experimental agent that targets ALK and mesenchymal-epithelial transition (MET) kinases and it is not currently approved by any regulatory agency. Pfizer's trial of crizotinib has demonstrated a high response rate (57%) in the *ALK* fusion-positive NSCLC population, indicating that these tumors have strong addiction exclusive to this oncokinase.[4] The three patients reported herein were all treated as part of the Pfizer trial after they had met the eligibility criteria and provided informed consent. All three patients showed a substantial responses to crizotinib. Although a minority of NSCLC arises from the *ALK* fusion-type oncokinase, most of ALK-positive NSCLC occur in younger people.[7] Thus, it is encouraging that ALK inhibitors will become available for use in the clinical setting. Moreover, crizotinib is also attractive as a potent ''pain killer'' because it was so effective against the pain produced by the bone metastases in Case 2 as to completely relieve the patient's cancer-related pain.

As for safety, temporary Grade 1 nausea and diarrhea were observed in all three patients and Grade 1 constipation coexisted in Case 2. Grade 1 dysgeusia of hot taste and visual disturbances (transient persistence of vision spectrum noted on moving from the dark to the light) occurred in Cases 2 and 3. These adverse events, except for dysgeusia, were reported in the trial[4] and all were tolerable. Crizotinib did not affect liver function, renal function, or blood cell counts in the three cases reported here.

Some responders (including two cases in the present study) develop resistance to crizotinib after a certain period, similar to most responders to EGFR tyrosine kinase inhibitors. This is a serious issue not to be overlooked. Based on the occurrence (Case 1) and unresponsiveness (Case 2) of brain metastases, crizotinib may not fully penetrate from the bloodstream into the CNS at the dose given in this trial. Costa *et al.*[11] recently reported a similar case to Case 1 in the present study, in whom the concentration of crizotinib was much lower in the cerebrospinal fluid (CSF) than in the plasma (0.0014 *vs.* 0.53 mol/L, respectively). Costa *et al.*[11] suggested that the low CSF:plasma ratio (0.0026) implied poor blood–brain barrier penetration of crizotinib, which may explain the persistent systemic disease control with crizotinib but the concurrent appearance of brain metastases.

Furthermore, two *de novo* mutations in the tyrosine kinase domain of *ALK* cDNA (G4374A and C4493A) have been identified recently from a patient who showed resistance to crizotinib.[12] These mutations result in substitutions of cysteine to tyrosine (C → Y) and leucine to methionine (L → M) at positions corresponding to amino acids 1156 and 1196, respectively. The L1196 of ALK corresponds to threonine (T) at position T315 in ABL and T790 in EGFR, the most frequently substituted position conferring resistance to inhibitors for these kinases. Conversely, C1156Y located adjacent to the αC helix on the N-terminal side has been proposed to allosterically hinder the binding of ALK inhibitors.[12] Such resistant mutations may provide another explanation for the lack of a response of brain metastases to crizotinib. Regarding the hepatic metastases in Case 2, it is unlikely that the hepatocyte growth factor/MET pathway or *MET* amplification (known resistant mechanisms for EGFR inhibitors) participated in this setting because crizotinib is a dual inhibitor for both ALK and MET kinases. We must investigate the mechanisms underlying the resistance to crizotinib to develop new treatment strategies, as well as second-generation ALK inhibitors, to overcome resistance.

Acknowledgments

The authors thank the three patients for consenting to the publication of their clinical details. The authors are also grateful to Dr Yung-Jue Bang and the medical staff of Seoul National University Hospital (Seoul, Korea) for their support in the treatment of these patients.

Disclosure Statement

KT has acted in an advisory role for Chugai Pharmaceutical Co., Ltd (Tokyo, Japan). The other authors report no potential conflicts of interest. None of the authors was an investigator in the trial conducted by Pfizer.

References

1 Takeuchi K, Choi YL, Togashi Y *et al.* KIF5B-ALK, a novel fusion oncokinase identified by an immunohistochemistry-based diagnostic system for ALK-positive lung cancer. *Clin Cancer Res* 2009; **15**: 3143–9.
2 Sakairi Y, Nakajima T, Yasufuku K *et al.* EML4-ALK fusion gene assessment using metastatic lymph node samples obtained by endobronchial ultrasound-guided transbronchial needle aspiration. *Clin Cancer Res* 2010; **16**: 4938–45.
3 Takeuchi K, Choi YL, Soda M *et al.* Multiplex reverse transcription-PCR screening for EML4-ALK fusion transcripts. *Clin Cancer Res* 2008; **14**: 6618–24.
4 Kwak EL, Bang YJ, Camidge DR *et al.* Anaplastic lymphoma kinase inhibition in non-small-cell lung cancer. *N Engl J Med* 2010; **363**: 1693–703.
5 Soda M, Choi YL, Enomoto M *et al.* Identification of the transforming EML4-ALK fusion gene in non-small-cell lung cancer. *Nature* 2007; **448**: 561–6.
6 Inamura K, Takeuchi K, Togashi Y *et al.* EML4-ALK fusion is linked to histological characteristics in a subset of lung cancers. *J Thorac Oncol* 2008; **3**: 13–7.
7 Inamura K, Takeuchi K, Togashi Y *et al.* EML4-ALK lung cancers are characterized by rare other mutations, a TTF-1 cell lineage, an acinar histology, and young onset. *Mod Pathol* 2009; **22**: 508–15.
8 Soda M, Takada S, Takeuchi K *et al.* A mouse model for EML4-ALK-positive lung cancer. *Proc Natl Acad Sci USA* 2008; **105**: 19893–7.
9 Choi YL, Takeuchi K, Soda M *et al.* Identification of novel isoforms of the EML4-ALK transforming gene in non-small cell lung cancer. *Cancer Res* 2008; **68**: 4971–6.
10 Koivunen JP, Mermel C, Zejnullahu K *et al.* EML4-ALK fusion gene and efficacy of an ALK kinase inhibitor in lung cancer. *Clin Cancer Res* 2008; **14**: 4275–83.
11 Costa DB, Kobayashi S, Pandya SS *et al.* CSF Concentration of the anaplastic lymphoma kinase inhibitor crizotinib. *J Clin Oncol* 2011; doi:10.1200/JCO.2010.34.1313 [Epub ahead of print].
12 Choi YL, Soda M, Yamashita Y *et al.* EML4-ALK mutations in lung cancer that confer resistance to ALK inhibitors. *N Engl J Med* 2010; **363**: 1734–9.

doi: 10.1111/j.1349-7006.2011.01970.x

Clinical Cancer Research

Pulmonary Inflammatory Myofibroblastic Tumor Expressing a Novel Fusion, PPFIBP1–ALK: Reappraisal of Anti-ALK Immunohistochemistry as a Tool for Novel ALK Fusion Identification

Kengo Takeuchi[1,2], Manabu Soda[4], Yuki Togashi[1,2], Emiko Sugawara[1,5], Satoko Hatano[1,2], Reimi Asaka[1,2], Sakae Okumura[3], Ken Nakagawa[3], Hiroyuki Mano[4,6], and Yuichi Ishikawa[2]

Abstract

Purpose: The anaplastic lymphoma kinase (ALK) inhibitor crizotinib has been used in patients with lung cancer or inflammatory myofibroblastic tumor (IMT), both types harboring ALK fusions. However, detection of some ALK fusions is problematic with conventional anti-ALK immunohistochemistry because of their low expression. By using sensitive immunohistochemistry, therefore, we reassessed "ALK-negative" IMT cases defined with conventional immunohistochemistry (approximately 50% of all examined cases).

Experimental Design: Two cases of ALK-negative IMT defined with conventional anti-ALK immunohistochemistry were further analyzed with sensitive immunohistochemistry [the intercalated antibody-enhanced polymer (iAEP) method].

Results: The two "ALK-negative" IMTs were found positive for anti-ALK immunohistochemistry with the iAEP method. 5′-rapid amplification of cDNA ends identified a novel partner of ALK fusion, protein-tyrosine phosphatase, receptor-type, F polypeptide-interacting protein-binding protein 1 (PPFIBP1) in one case. The presence of PPFIBP1–ALK fusion was confirmed with reverse transcriptase PCR, genomic PCR, and FISH. We confirmed the transforming activities of PPFIBP1–ALK with a focus formation assay and an *in vivo* tumorigenicity assay by using 3T3 fibroblasts infected with a recombinant retrovirus encoding PPFIBP1–ALK. Surprisingly, the fusion was also detected by FISH in the other case.

Conclusions: Sensitive immunohistochemical methods such as iAEP will broaden the potential value of immunohistochemistry. The current ALK positivity rate in IMT should be reassessed with a more highly sensitive method such as iAEP to accurately identify those patients who might benefit from ALK-inhibitor therapies. Novel ALK fusions are being identified in various tumors in addition to IMT, and thus a reassessment of other "ALK-negative" cancers may be required in the forthcoming era of ALK-inhibitor therapy. *Clin Cancer Res; 17(10); 3341–8. ©2011 AACR.*

Introduction

Anaplastic lymphoma kinase (ALK) is a receptor tyrosine kinase that was discovered in anaplastic large cell lymphoma (ALCL) in the form of a fusion protein, NPM–ALK. (1, 2). In addition to ALCL (fused to NPM, TPM3, TPM4, ATIC, TFG, CLTC, MSN, MYH9, or ALO17; refs. 1–10), ALK has further been found to generate fusions in inflammatory myofibroblastic tumor (IMT; TPM3, TPM4, CLTC, CARS, RANBP2, ATIC, or SEC31L1; refs. 10–15), ALK-positive large B-cell lymphoma (CLTC, NPM, SEC31L1, or SQSTM1; 16–19), lung cancer (EML4 or KIF5B; refs. 20, 21), and ALK-positive histiocytosis (TPM3; ref. 22) Besides, some ALK fusions have been reported without showing histopathologic evidence: TPM4–ALK in esophageal squamous cell carcinoma (23, 24), TFG–ALK in lung adenocarcinoma (25), and EML4–ALK in colon and breast carcinomas (26). The wild-type ALK is mainly expressed in the developing nervous system, and is usually not expressed in other normal tissues (27). A fusion protein formation with a partner through chromosomal translocations is the most common mechanism of ALK overexpression and ALK kinase domain activation. These features render ALK fusion oncokinase an ideal molecular target.

Recently, the ALK inhibitor crizotinib has been used in patients with lung cancer or IMT, both types harboring ALK fusions (28, 29). The compound showed a 57% response rate in lung cancers (28), and a strong response for several months in IMT (29). Crizotinib and other ALK inhibitors

Authors' Affiliations: [1]Pathology Project for Molecular Targets; [2]Division of Pathology; and [3]Department of Thoracic Surgical Oncology, Thoracic Center, Cancer Institute Hospital, Japanese Foundation for Cancer Research, Tokyo; [4]Division of Functional Genomics, Jichi Medical University, Tochigi; [5]Department of Comprehensive Pathology, Graduate School, Tokyo Medical and Dental University; and [6]Department of Medical Genomics, Graduate School of Medicine, University of Tokyo, Tokyo, Japan

Note: Supplementary data for this article are available at Clinical Cancer Research Online (http://clincancerres.aacrjournals.org/).

Corresponding Author: Kengo Takeuchi, Pathology Project for Molecular Targets, The Cancer Institute, Japanese Foundation for Cancer Research, Tokyo 135-8550, Japan. Phone: +8133-520-0111; Fax: +8133-570-0230; E-mail: kentakeuchi-tky@umin.net

doi: 10.1158/1078-0432.CCR-11-0063

Translational Relevance

Anaplastic lymphoma kinase (ALK) inhibitors have become one of the most promising groups of molecularly targeted drugs. Therefore, ALK is no longer a mere research target or simply a diagnostic marker, but is directly linked to the therapeutic benefit of patients harboring the fusions.

Pathologic diagnoses for ALK fusion-positive tumors have been made reliably with anti-ALK immunohistochemistry. Since the discovery of EML4–ALK, however, an unexpected problem in anti-ALK immunohistochemistry has become apparent, that is, the inability to detect a low level of EML4–ALK expression. To overcome this, we developed the intercalated antibody-enhanced polymer immunohistochemistry, which successfully detected EML4–ALK.

In other words, this indicates that unknown ALK fusions, particularly those expressed at a low level, may wait to be discovered in "ALK-negative" tumors defined with conventional immunohistochemistry. In the forthcoming era of ALK-inhibitor therapy, "ALK-negative" tumors should be reassessed with a high sensitive immunohistochemistry and, if positive, be further examined with appropriate molecular method(s).

have thus become one of the most promising groups of molecularly targeted drugs. Therefore, the sensitive and accurate identification of ALK fusion in tumors has also become clinically relevant, because it is no longer a mere research target or simply a diagnostic marker, but is directly linked to the therapeutic benefit of patients harboring the fusions.

Identification of such ALK fusions, especially within ALCL, has been prompted by the immunohistochemical staining pattern with antibodies to ALK. In ALCL, the most common ALK fusion is NPM–ALK (comprising approximately 80% of all cases), and its immunohistochemical staining pattern is both nuclear and cytoplasmic. NPM has a nuclear localization signal in the C-terminal region, and therefore the heterodimers of wild-type NPM with NPM–ALK fusion protein are transported to the nucleus whereas NPM–ALK homodimers remain within the cytoplasm (30). In contrast, other fusions do not localize in the nucleus and do not show a nuclear staining pattern in anti-ALK immunohistochemistry. Interestingly, each ALK fusion usually has its own characteristic anti-ALK immunohistochemical staining pattern, because the subcellular localization of ALK fusions is dependent on the corresponding fusion partners. Anti-ALK immunohistochemistry has thus become a highly useful tool for both research and diagnostic purposes.

Since the discovery of EML4–ALK fusion in lung cancer (20), however, an unexpected problem in anti-ALK immunohistochemistry has become apparent, that is, the inability to detect a low level of fusion expression. To overcome this, we developed the intercalated antibody-enhanced polymer (iAEP) method, which moderately raises sensitivity in the immunohistochemical detection system (21). With this very simple method, anti-ALK immunohistochemistry has become a potent weapon in the diagnosis of EML4–ALK-positive lung cancer (21, 31–33). Other researchers used an anti-ALK rabbit monoclonal antibody, which is usually more sensitive than mouse monoclonal antibody, which can stain EML4–ALK (34). However, most EML4–ALK-positive lung cancer tissues do not stain well with conventional anti-ALK immunohistochemical methods because of the low message/protein level of EML4–ALK (21, 35). The expression level of a fusion gene depends on the promoter activity of the 5′-side gene, and that of EML4 is likely to be lower than that of the other ALK fusion partner genes, which may explain why EML4–ALK had not been discovered until 12 years after the development of the first anti-ALK antibody became available for immunohistochemistry (36). In other words, a tumor that immunostains for ALK only by a sensitive immunohistochemistry method may harbor a novel ALK fusion. Interestingly, in this study, we detected 2 IMT cases positive for ALK immunohistochemistry only when stained by iAEP method (21), and successfully identified a novel fusion gene, protein-tyrosine phosphatase, receptor-type, F polypeptide-interacting protein-binding protein 1 (PPFIBP1)–ALK.

Materials and Methods

Materials

Pathologic specimens from 2 pulmonary IMT cases, originally diagnosed as fibrous histiocytoma (1988: case 1, 45-year-old male; 1998: case 2, 34-year-old female), were reassessed morphologically and immunohistochemically. Surgically removed tumor specimens were routinely fixed in 20% neutralized formalin and embedded in paraffin for conventional histopathologic examination. For case 2, total RNA was extracted from the corresponding snap-frozen specimen and purified with the use of an RNeasy Mini kit (Qiagen). The study was approved by the institutional review board of the Japanese Foundation for Cancer Research.

Immunohistochemistry

Formalin-fixed, paraffin-embedded tissue was sliced at a thickness of 4 μm, and the sections were placed on silane-coated slides. For antigen retrieval, the slides were heated for 40 min at 97°C in Target Retrieval Solution (pH 9.0; Dako). For the conventional staining procedure, the slides were incubated at room temperature with Protein Block Serum-free Ready-to-Use solution (Dako) for 10 minutes and then with primary antibodies against ALK (5A4), smooth muscle actin, muscle-specific actin (HHF35), CD34, cytokeratins (AE1/AE3), S100, or desmin for 30 minutes. The immune complexes were then detected with dextran polymer reagent (EnVision + DAB system; Dako) and an AutoStainer instrument (Dako). The iAEP method was also used for the sensitive detection of ALK, as described previously (21).